Journal of Human Evolution 55 (2008) 817–833

Contents lists available at ScienceDirect

Journal of Human Evolution

journal homepage: www.elsevier.com/locate/jhevol

Dating the demise: Neandertal extinction and the establishment of modern humans in the southern Caucasus

Daniel S. Adler [a,*], Ofer Bar-Yosef [b], Anna Belfer-Cohen [c], Nicholas Tushabramishvili [d], E. Boaretto [e,f], N. Mercier [g], H. Valladas [h], W.J. Rink [i]

[a] Department of Anthropology, 354 Mansfield Road, Unit 2176, University of Connecticut, Storrs, CT 06269-2176, USA
[b] Harvard University, Department of Anthropology, Peabody Museum, 11 Divinity Ave., Cambridge, MA 02138, USA
[c] Institute of Archaeology, Hebrew University, Mt. Scopus, Jerusalem, 91905, Israel
[d] Georgian National Museum, 3 Rustaveli Ave., 0105 Tbilisi, Georgia
[e] Radiocarbon Dating and Cosmogenic Lab, Kimmel Center for Archaeological Science, Weizmann Institute of Science, 76100 Rehovot, Israel
[f] Department of Land of Israel Studies and Archaeology, Bar Ilan University, 52900 Ramat Gan, Israel
[g] Institut de recherche sur les Archéomatériaux, UMR 5060, CNRS – Univ. Bx3, Centre de Recherche en Physique Appliquée à l'Archéologie (CRPAA), Maison de l'archéologie, 33607 Pessac cedex, France
[h] Laboratoire des Sciences du Climat et de l'Environnement, Domaine du CNRS, Avenue de la Terrasse – Bat. 12, 91198 Gif sur Yvette, France
[i] School of Geography and Earth Sciences, McMaster University, 1280 Main St. West, Hamilton, Ontario, Canada L8S 4K1

ARTICLE INFO

Article history:
Received 9 September 2007
Accepted 25 November 2007

Keywords:
Chronometric dating
Discard protocol
Middle to Upper Paleolithic replacement event

ABSTRACT

This paper considers the recent radiometric dating (^{14}C-AMS, TL, ESR) of 76 late Middle and early Upper Paleolithic samples from Ortvale Klde Rockshelter, located in the Republic of Georgia. We present a critical evaluation of each date based on its stratigraphic and archaeological context, its pretreatment and contamination history, and its resulting accuracy and precision, the goal being to establish a sound chronology for the site. Only by systematically identifying aberrant dates within a data set and isolating them from further analysis can we hope to understand cultural and biological phenomena on an accurate temporal scale. Based on the strict discard protocol outlined here, we omit 25% of the dated samples from the analysis. The remaining data speak to the lengthy tenure of Neandertals in the region, but also to their relatively rapid demise and the establishment of modern human populations ~38–34 ka ^{14}C BP (42–39 ka cal BP_{Hulu}). We compare these chronometric data with those from the neighboring sites of Bronze and Dzudzuana caves, as well as Mezmaiskaya Cave, located in the northern Caucasus. While the lack of key contextual information limit our ability to subject these other data sets to the same critical evaluation procedure, they provide the first interregional temporal assessment of the Middle to Upper Paleolithic "transition," the results of which suggest an initial expansion of modern humans into the southern Caucasus followed by expansion along the Black Sea coast and into the northern Caucasus.

Introduction

Models concerning the speed and geographic course of the shift from the Middle to the Upper Paleolithic across Eurasia (e.g., Bocquet-Appel and Demars, 2000; Conard and Bolus, 2003; Anikovich et al., 2007), commonly understood as the biological and cultural replacement of Neandertals by modern humans (Bar-Yosef, 1998, 2001; but see Zilhão and d'Errico, 1999; d'Errico, 2003; Zilhão, 2006), rely to a large degree on a combination of chronometric records from individual archaeological sites and, when appropriate, the calibration of these records. However, such records are continually in flux and subject to reinterpretation as new site-specific chronometric data become available and as the dating techniques themselves evolve (e.g., AMS "ultrafiltration" pre-treatment: Bronk Ramsey et al., 2004; Higham et al., 2006b; Fourier transform infrared Spectroscopy: Yizhaq et al., 2005). Both of these factors contribute greatly to the periodic rewriting/revision of prehistory (e.g., Higham et al., 2006a; Jacobi and Higham, 2008). But perhaps the single most important issue regarding the testing of demographic and behavioral models, such as those relating to the end of the Middle and beginning of the Upper Paleolithic, is the actual quality and reliability of the samples that comprise the individual chronometric records against which hypotheses are tested. Too often researchers accept all chronometric data as of equal quality and reliability, or worse, they reject without explanation

* Corresponding author.
E-mail addresses: daniel.adler@uconn.edu (D.S. Adler), obaryos@fas.harvard.edu (O. Bar-Yosef), belferac@mscc.huji.ac.il (A. Belfer-Cohen), nikatushi@hotmail.com (N. Tushabramishvili), elisabetta.boaretto@weizmann.ac.il (E. Boaretto), Norbert.-Mercier@u-bordeaux3.fr (H. Mercier), helene.valladas@lsce.cnrs-gif.fr (H. Valladas), rinkwj@mcmaster.ca (W.J. Rink).

0047-2484/$ – see front matter © 2008 Elsevier Ltd. All rights reserved.
doi:10.1016/j.jhevol.2008.08.010

chronometric data that do not fit their a priori assumptions. This situation can only be rectified by the systematic analysis and publication of all chronometric data from a given site in which researchers are open and specific about the archaeological context and association of each dated sample, and their criteria for accepting or rejecting individual age determinations. Although progress has been made in this direction (e.g., Spriggs, 1989; Spriggs and Anderson, 1993; Pettitt et al., 2003; Millard, 2008), cases are rare and the true nature of many chronometric records, and thus the demographic and behavioral processes they chart, remains elusive, in particular with respect to the shift from the Middle to the Upper Paleolithic.

In this paper we attempt to clarify the chronometric situation at one site in the southern Caucasus, Ortvale Klde, where late Middle and early Upper Paleolithic deposits have been carefully excavated and dated using a variety of chronometric methods. Prior to the implementation of an integrated dating program at Ortvale Klde, only a handful of radiometric, mostly conventional ^{14}C readings, were available for the entire Republic of Georgia (Tushabramishvili, 1978; Liubin et al., 1985; Lioubine, 2002). It has been impossible, therefore, to relate sites temporally or culturally unless one relies on coarse-grained lithic typologies and assumed climatic correlations (e.g., Doronichev, 1993; Cohen and Stepanchuk, 1999; Golovanova and Doronichev, 2003; see Adler and Tushabramishvili, 2004 for discussion). With the recent dating of Ortvale Klde, a measure of clarity has been introduced to an otherwise murky picture of prehistoric development within the region. But as with any other archaeological site the individual chronometric data from Ortvale Klde are not always stratigraphically consistent and each data point must be subjected to critical analysis. In this paper we present background information on Ortvale Klde followed by an assessment of the archaeological and stratigraphic context of the dated samples. We introduce a discard protocol against which the dated samples from each layer are assessed for their reliability and either retained for, or rejected from, further analysis. The remaining data are then correlated with paleoclimatic proxies and compared with chronometric records from the neighboring sites of Bronze and Dzudzuana caves. We conclude with a discussion of these regional data in light of recent dating efforts at Mezmaiskaya Cave and what these chronologies indicate about the Neandertal occupation of the Caucasus and the timing of their eventual demise.

Ortvale Klde

Ortvale Klde is located outside the town of Chiatura, approximately 35 meters (m) above the west bank of the Cherula River (ca. 530 meters above sea level, m.a.s.l.), a tributary of the Kvirila River that flows into the Black Sea via the Rioni River. The site is a karstic rockshelter composed of Cretaceous limestone with two chambers opening to the east. Within the small southern chamber and along the slope D. Tushabramishvili and N. Tushabramishvili excavated over 40 m^2 (Tushabramishvili et al., 1999). All of the data presented here derive from the new excavations that were conducted in this portion of the rockshelter; the results of earlier excavations are summarized elsewhere (Adler, 2002; Adler and Tushabramishvili, 2004).

The new excavations at Ortvale Klde, conducted from 1997–2001, focused on 6 m^2 and led to the recovery of over 12,000 early Upper Paleolithic (EUP) and 22,000 late Middle Paleolithic (LMP) stone artifacts from Layers 2–4 and Layers 5–7, respectively (Fig. 1).

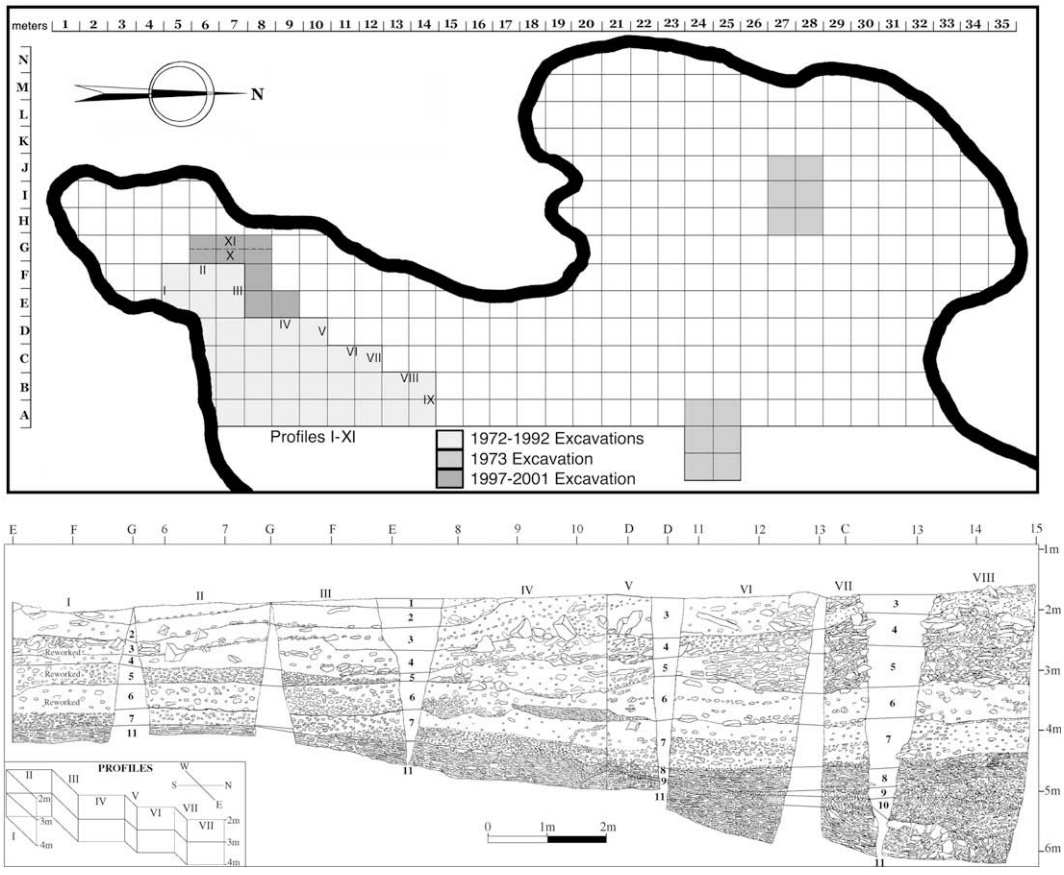

Fig. 1. Top: plan view of Ortvale Klde with documented profiles (I-XI) and areas and seasons of excavation. Bottom: composite profile of Ortvale Klde with Layers 1–11 and Profiles I-XI.

More than 3,200 EUP and 12,500 LMP faunal specimens were also recovered (Bar-Oz and Adler, 2005; Adler et al., 2006a). The lithic assemblage from the earliest EUP (Layers 4d and 4c) contains unidirectional blade cores, end scrapers on blades, rounded flake scrapers, burins on truncation, numerous retouched bladelets (some 2–3 mm wide), and backed bladelets (Fig. 2; Adler et al., 2006b; Bar-Yosef et al., 2006). The majority of these items were produced on locally available flint, but a significant portion of the assemblage was produced on obsidian available ≥100 km to the southeast. Three bevel-based bone/antler points, two polished bone/antler abraders, and a polished bone implement with parallel linear incisions were also recovered. Similar lithic and bone materials were never encountered in the underlying LMP layers, which are dominated by Levallois technology and a typical array of Middle Paleolithic scraper types produced almost exclusively on local flint (Fig. 3; Adler, 2002; Adler et al., 2006a,b). Rare Mousterian artifacts were encountered at the contact between the LMP and EUP but these were easily distinguished by their patination and typology (Adler, 2002). During both the LMP and EUP, the site's occupants focused on the acquisition of *Capra caucasica* during this taxon's seasonal migration (late fall–early spring) into the area from higher elevations (Adler et al., 2006a). Ortvale Klde currently represents the only well excavated and dated LMP–EUP locality in the southern Caucasus and a variety of studies suggest that Neandertals and modern humans did not coexist in the region for any appreciable period of time, if at all (Adler, 2002; Bar-Oz and Adler, 2005; Adler et al., 2006a,b; Bar-Yosef et al., 2006).

Between 1999 and 2001, 165 chronometric dating samples were collected from Ortvale Klde and submitted for analysis by accelerator mass spectrometry (AMS), thermoluminescence (TL), and electron spin resonance (ESR) (Table 1). Of these samples, 76 (46.1%) have been successfully dated by the Weizmann Institute of Science (Israel), the National Science Foundation AMS Laboratory in Arizona (USA), the Laboratoire des Sciences du Climat et de

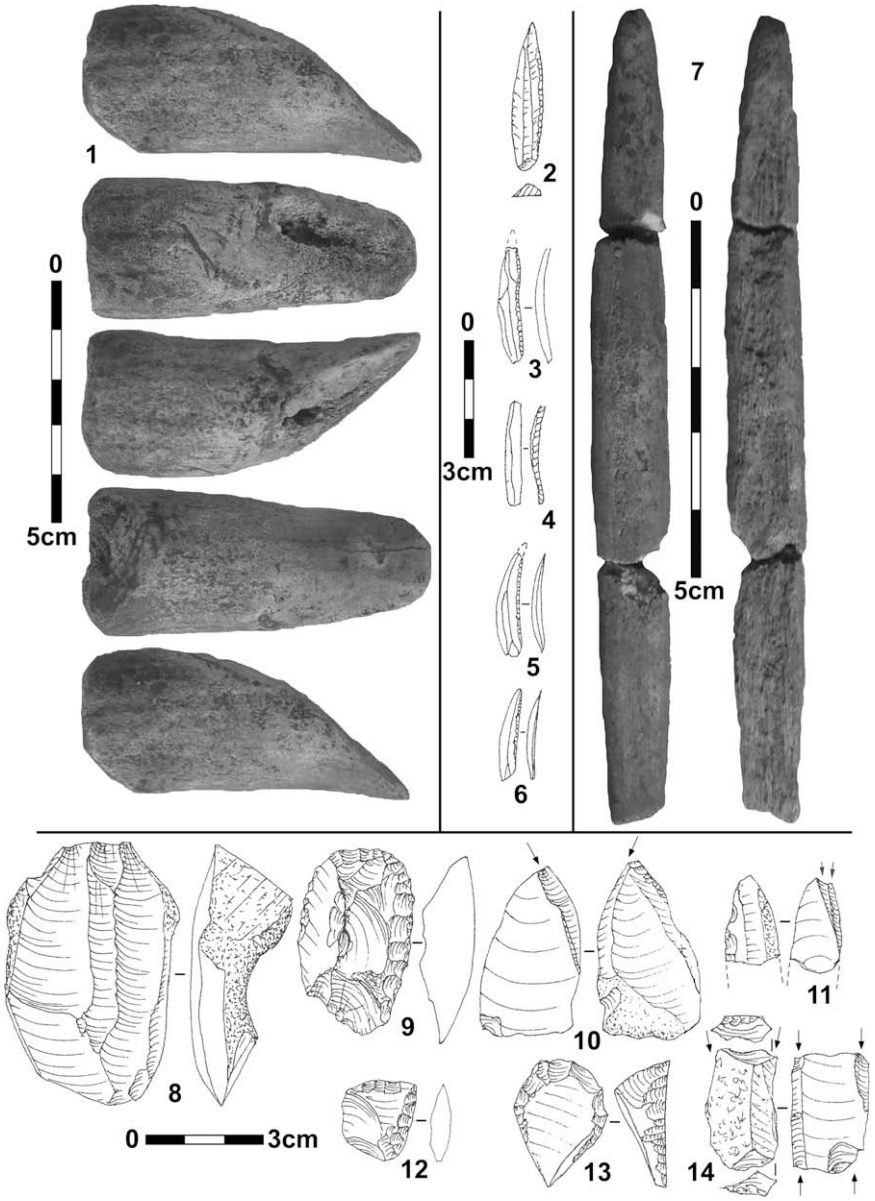

Fig. 2. Upper Paleolithic artifacts from Ortvale Klde: 1) five views of an antler abrader; 2–6) retouched and backed bladelets; 7) two views of a bone/antler point; 8) unidirectional blade core; 9) oval scraper on flake; 10) burin on oblique truncation; 11) burin on bulbar face on broken blade; 12) atypical "thumb-nail scraper;" 13) end scraper on retouched flake; 14) quadruple burin on truncation (burned); [2–6, 8–10, 13–15) flint; 11) obsidian; 8) Layer 3; 1–7, 9–11, 13–14) Layer 4c; 12) Layer 4d]. Illustrations by O. Bar-Yosef and photographs by D. S. Adler. Modified after Adler et al. (2006b).

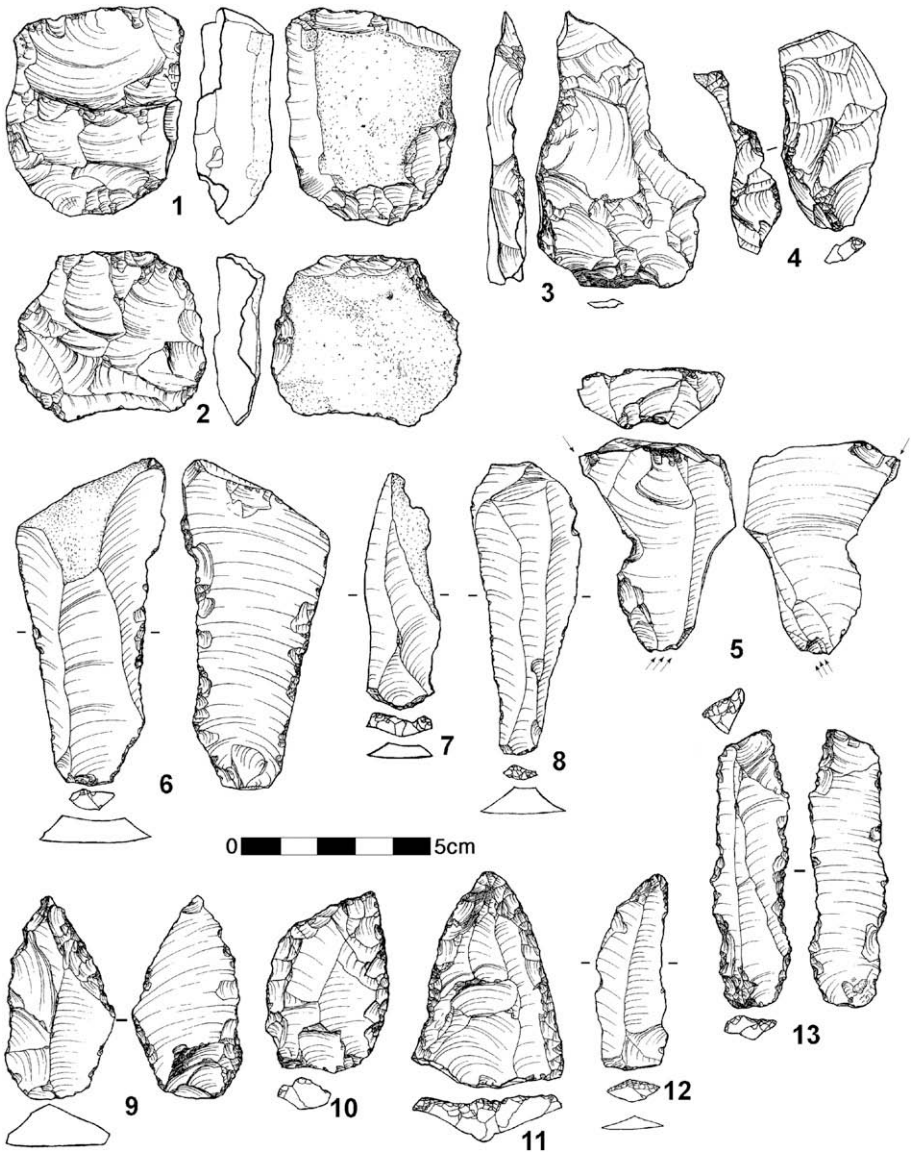

Fig. 3. Middle Paleolithic artifacts from Ortvale Klde: 1–2) unidirectional Levallois cores with distal and lateral trimming; 3–4) "prepared" débordants; 5) eclat outrepassé (burin); 6–8) unidirectional blades; 9) utilized single scraper with ventrally thinned base; 10) déjeté scraper; 11) convergent scraper; 12) retouched blade; 13) utilized double scraper with ventral retouch [1–13) flint; 1–2) Layer 10; 3, 5, 9–11, 13) Layer 5; 4, 6–8) Layer 9; 12) Layer 10]. Illustrated by J. Skidel-Rymar. Modified after Adler (2002).

Table 1
The stratigraphic context and frequency of all dating samples analyzed from Ortvale Klde[a]

	Layer	AMS		TL Flint	ESR Teeth	Total Samples	Dated Samples [%]
		Bone	Charcoal				
EUP	2	4 (2)	2 (0)	0	0	6	2 [33.3]
	2&3	0	3 (0)	0	0	3	0
	3	3 (0)	3 (2)	0	0	6	2 [33.3]
	4a	0	2 (0)	0	0	2	0
	4b	2 (2)	1 (1)	0	0	3	3 [100]
	4c	6 (0)	18 (15)	16 (5)	0	40	19 [47.5]
	4d	3 (3)	0	0	0	3	3 [100]
LMP	5	10 (4)	1 (0)	6 (5)	0	17	9 [52.9]
	6	17 (1)	19 (8)	4 (4)	0	40	13 [32.5]
	7	5 (2)	4 (2)	9 (9)	6 (5)	24	18 [75.0]
	8	0	0	0	0	0	0
	9	0	0	10 (2)	0	10	2 [20.0]
	10	0	0	11 (5)	0	11	5 [45.5]
	Total	50 (14)	53 (28)	56 (29)	6 (5)	165	76 [46.1]

[a] Samples whose precise stratigraphic position within either Layer 2 or Layer 3 could not be determined were classified as "Layer 2/3". Parenthetical data represent actual samples dated. All samples were either excavated or collected, and packaged by D. S. Adler.

l'Environnement (France), and McMaster University (Canada). All samples submitted for dating were excavated on site or selected from Georgian State Museum collections by D. S. Adler following the specific collection and packaging criteria provided by the participating laboratories. Specific archaeological, stratigraphic, and contextual information was recorded for each sample collected in the field while the archaeological context of museum materials was crosschecked for consistency against artifact labels, museum inventories, and excavation notes. The materials submitted for dating include bone collagen and charcoal for AMS, burned flints for TL, and ungulate teeth for ESR (Table 1).

Stratigraphic and archaeological context of the Ortvale Klde samples

Previous work in the southern chamber of Ortvale Klde identified 11 lithostratigraphic layers of which two were assigned to the Upper Paleolithic and seven to the Middle Paleolithic (Tushabramishvili, 1994; Tushabramishvili et al., 1999). Of particular importance was the identification of a "transitional" industry composed of Middle and Upper Paleolithic stone tools previously thought to represent a local MP–UP "transition." New excavations at the site revealed several discrepancies with the original stratigraphic designations related to the association of specific lithostratigraphic layers with particular archaeological cultures (see Adler, 2002; Adler et al., 2006a). We did not find any evidence for an in situ cultural "transition" between the Middle and Upper Paleolithic, but instead identified a distinct archaeological, stratigraphic, and temporal break between Layer 5 (LMP) and Layer 4d (EUP), which highlights the abrupt stratigraphic and temporal disappearance of the LMP and intrusive nature of the EUP. Therefore, we interpret these data not as evidence for a "transition," in which one would expect to find intermediate forms, be they fossil or archaeological, but rather for population replacement. The following provides a brief accounting of the stratigraphic and archaeological context of Ortvale Klde and the chronometric specimens collected there.

Layers 2–3 (EUP)

Recent excavations at Ortvale Klde identified a clear stratigraphic boundary between Layers 2 and 3 defined by dense concentrations of large (~50 cm) limestone slabs and small blocks of éboulis (5–10 cm) that formed a 5–10 cm thick barrier (Fig. 4). These limestone platforms had a flat orientation and smaller blocks of éboulis filled gaps between individual slabs, providing little room for material to migrate between layers. Still, clear signs of bioturbation in the form of ancient rodent and insect burrows were observed within Layer 3, but similar features were not identified in Layer 4a and below. Within Layer 2, find densities are extremely low except at the base of the layer just above the limestone platform separating the deposit from Layer 3 (Fig. 4). The opposite was observed in Layer 3 where find densities are highest just below this platform but decrease dramatically with depth, the last 10 cm of Layer 3 being almost completely sterile. An extensive deposit of light gray ash underlies the entire limestone platform dividing Layers 2 and 3 (Fig. 4).

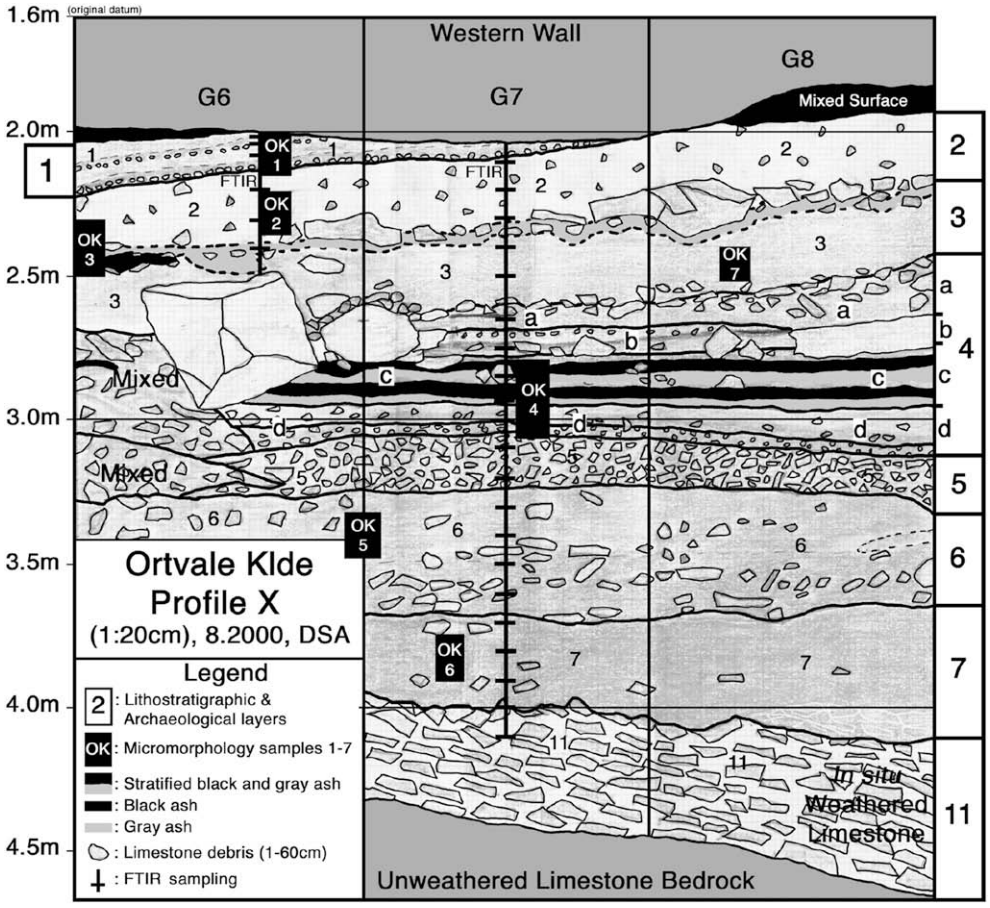

Fig. 4. Profile X after the excavation of sub-squares "a" and "c" (unexcavated sub-squares "b" and "d" pictured) with Layers 1-7 and 11 and sub-layers 4a–d. See Fig. 1 for the location of Profile X. Note that samples OK3 (Profile II), OK5 (Profile II), and OK7 (Profile XI) are placed on Profile X for convenience. Their actual positions with reference to Profile X, and as indicated by their profile designations, are OK3 + 50 cm east, OK5 + 50 cm east, and OK7 + 50 cm west.

Layer 4a–d (EUP)

In total, Layer 4 spans approximately 65 cm in the vertical dimension (Fig. 4). Within Layer 4, four distinct sub-layers (a–d) were discerned and traced across all of the excavation units and into adjacent sections (Fig. 4). Each sub-layer was excavated individually, thus increasing the stratigraphic control of the archaeological and chronometric material recovered. Two clear sub-layers were defined by fine laminations (4b) and loose yellow sediments immediately below the limestone éboulis contact with Layer 3 (4a). Find densities were low within Layers 4a and 4b, and another dense deposit of éboulis defines the base of Layer 4b. Within Layer 4c a series of stratified black and gray ash lenses contain a rich lithic and faunal assemblage. Given the spatial extent of these ash lenses and their degree of lamination and stratigraphic integrity, it is likely that they were re-deposited via colluvial or aeolian forces (but not fluvial, see Adler, 2002). Micromorphological analyses by P. Goldberg and C. Mallol identified well-preserved fragments of bone and charcoal, suggesting they were not transported great distances or exposed on the surface for extended periods of time. However, the presence of very small fragments of burned and unburned bone mixed together suggests that some lateral movement occurred. Therefore, it is likely that the main areas of combustion were located elsewhere, perhaps near the front of the rockshelter. Finally, some portions of the sampled sediments are bioturbated, displaying a porous, aggregated microstructure. The Upper Paleolithic sequence originates with Layer 4d, which is deposited directly atop Layer 5 (LMP) and terminates at the contact with the ash deposits of Layer 4c (Fig. 4). Layer 4d is composed of a soft brown, gray ash matrix that fills the gaps between the dense accumulations of small limestone éboulis constituting Layer 5. A scooped out hearth, ringed by large fire-cracked limestone blocks, was discovered within Layer 4d directly atop Layer 5. This hearth, containing numerous burned backed microliths of flint and obsidian and dense accumulations of fine-grained dark gray ash likely signals one of the first EUP occupations of the site. This well-preserved feature indicates that Layer 4d does not contain evidence for the in situ "transition" from the Middle to the Upper Paleolithic, but rather the abrupt appearance of a full-fledged EUP culture. Since Layer 4d was deposited atop the terminal LMP surface, mixing between these two stratigraphic units cannot be ruled out even though such evidence was not encountered in the field or during subsequent analysis of the lithic materials.

Layer 5 (LMP)

Layer 5 represents the last LMP occupation at Ortvale Klde, and in this area of the site is composed of a dense accumulation of small (1–6 cm) éboulis, roughly 10–15 cm in thickness; the layer thickens considerably to the north (Fig. 1). The sediments and éboulis are very compact, and clay-rich material within the matrix acts to "cement" the deposit. Archaeologically the layer is very rich, but the lithic and faunal remains show traces of weathering, and the coarse surrounding matrix has damaged many of their edges.

Layers 6 and 7 (LMP)

Layer 6 is composed of a black, granular matrix containing very few clasts and underlies the éboulis-rich matrix of Layer 5. The sediments within Layer 6 are very rich in lithic, faunal, and organic material, in particular ash and charcoal, and the layer appears to have experienced considerable bioturbation probably resulting from extensive human and rodent activity. The layer is approximately 25 cm thick within the area of excavation, and there is very little evidence for internal stratification (Fig. 4). The contact between Layers 6 and 7 becomes increasingly difficult to discern as one moves north along the section. Layer 7 is also very rich in lithic, faunal, and organic remains. Within the area of excavation this layer represents the last archaeological horizon and is underlain by Layer 11, a dense structure of in situ weathered limestone that has not undergone lateral or vertical displacement. Given the evidence for bioturbation and human activity, we assume that the archaeological and radiometric materials from Layers 6 and 7 have experienced some movement.

Layer 8 (sterile) and Layers 9–10 (LMP)

Unit E10, located just north of the 1997–2001 excavation area, documents the southern termination of Layer 8 (Fig. 1). This deposit is composed of a dense, compact accumulation of éboulis and is devoid of sediment and archaeological material. Layer 8 is correlated with a period of increased éboulis deposition and temporary site abandonment perhaps linked to an environmental decline. Layers 9 and 10, located immediately below Layer 8, are composed of dense accumulations of éboulis. These layers are reported to have been extremely rich in archaeological material during previous excavations (Tushabramishvili et al., 1999), but close inspection of the remaining deposits indicated very low densities of material.

Discard protocol

Not all chronometric samples or age estimates are equal in quality, and each chronometric technique suffers to varying degrees from issues relating, but not limited to, archaeological context and stratigraphy, sample pretreatment and contamination, and accuracy and precision. To minimize the risk of including aberrant data in our analysis of Ortvale Klde we adhere to the discard protocol outlined below. While not identical to the procedures outlined by others, for example Spriggs (1989), Spriggs and Anderson (1993), Pettitt et al. (2003), or Millard (2008), our protocol shares many basic features and concerns in common and is similarly designed to cull dates that obscure otherwise robust temporal trends within the dataset. The omission of any given date from further analysis does not necessarily imply that we regard the specimen as incorrectly dated, but rather it indicates, after careful consideration, our lack of confidence in a specimen's analytical quality, archaeological context, and/or taphonomic history.

Stratigraphic and archaeological context

A sample is treated with caution if it is not in accord with the stratigraphic sequence, especially in cases where contacts between strata are well-defined and little evidence is found for mixing between layers. We appreciate the potentially severe impact of various taphonomic forces on the three-dimensional context of (especially small) datable materials within a stratigraphic sequence. Therefore, we place particular value on those specimens systematically collected and recorded during excavation and for whom a clear archaeological association has been established. A sample that is considerably too young or old (>2-sigma) given its stratigraphic position within a specific archaeological layer or strictly defined sub-layer, or whose archaeological or stratigraphic context is in question is omitted from further analysis. At Ortvale Klde these former restrictions were relaxed for artificially thick layers in which no internal stratification could be discerned (e.g., Layers 6 and 7).

Pretreatment and contamination

A sample is omitted from further analysis if it does not pass the specific pretreatment criteria of each chronometric technique and laboratory. Issues relating to pretreatment are of particular import

when considering AMS specimens as these are more prone to various forms of contamination, especially within the timeframes concerned here [i.e., >4 radiocarbon half-lives, (5,730 ± 40)].

Accuracy and precision

A sample is omitted from further analysis if it is reported as a minimum estimate (e.g., >45 ka ^{14}C BP). Ideally a range of dated samples is available from a given archaeological horizon or sub-layer therein. In such cases, we look to identify coherent, stratigraphically adjacent, statistically significant groups of dates as well as outliers. The latter are defined as samples that fall beyond 2-sigma of the weighted mean for the group; below this level there is a 95% probability that the actual age of the deposit has been bracketed. A series of weighted means are calculated for the specimens from each layer until a statistically significant grouping is attained (*t*-values <2.0 indicate that the data are identical at 2-sigma). It should be noted that we in no way expect an archaeological layer, deposited over perhaps thousands of years, to correspond to a single age, however, given the scale of the statistical uncertainties associated with Pleistocene radiometric estimates, we do expect, following the procedures outlined here, that the true depositional interval will be bracketed.

TL analysis

A total of 56 burned flints were submitted for TL analysis of which 29 (58%) produced results. The inability to date all specimens relates in part to the degree to which each specimen was heated in prehistory as well as its size (e.g., 2 mm are removed from each side of a specimen to avoid problems of microdosimetry, thus, many samples are too small to date following pretreatment). The TL method is based on the fact that burned flints are excellent natural dosimeters that record doses delivered by different types of radiation related to the decay of radioisotopes, such as the Uranium-series, Thorium-series, and Potassium within archaeological layers. The TL method is based on dosimetric measurements of these ionizing radiations. α and β particles emitted from radioisotopes within the flint itself provide an "internal dose." An "external dose" from long-range (~40 cm max.) γ-rays (as well as from cosmic radiations) requires careful consideration of the immediate environment of the dated pieces.

Sample preparation and pretreatment

At Ortvale Klde, 22 recently excavated flint artifacts and 7 curated specimens from previous excavations showing signs of heating were selected for analysis and prepared following an established protocol (Valladas, 1992). After the outermost 2 mm of each flint was removed, the remaining core was crushed and subjected to chemical treatment and its TL emission was analyzed. The technical results and age estimates are presented in Table 2 while the weighted means are presented in Table 3.

Based on the discard protocol outlined above only 3 TL specimens are omitted from the analysis; in comparison to their stratigraphic neighbors, GIF 12 (Layer 6) is considerably younger (>2 sigma), while GIF 22 and 25, derived from Layer 7, are older (>2 sigma). Otherwise the weighted means outlined in Table 3 and illustrated in Fig. 5 indicate that all other specimens pass our protocol and are in strong statistical agreement within their given layer. The large sigma values associated with each specimen reflect careful consideration of a variety of post-depositional factors such as a) the variability of the measured external dose rates that result from the radioactive heterogeneity of the sediments, b) the inability to determine the present dose rate of each specimen at the exact location of discovery, and c) fluctuating water content in the sediment.

The EUP and LMP deposits

Layer 4c produced very consistent results (33.3% of submitted samples measured) that suggest an age on the order of 28.9 ka BP_{TL} (Table 3). Six specimens from Layer 5 were submitted for analysis and four produced a weighted mean of 45.8 ka BP_{TL}. In both instances these results are considerably younger (Layer 4c) or older (Layer 5) than their associated AMS results. Unfortunately, this problem has not been resolved. Samples from Layer 6 have a weighted mean of 48.5 ka BP_{TL}, which when considered with reference to its associated sigma value, is in good agreement with the result from Layer 7 (43.4 ka BP_{TL}; Table 3; Fig. 5). All nine specimens from Layer 7 are derived from a ~7 cm-thick excavation spit within three sub-squares (a, b, and d) of Unit E8 (Fig. 1), thus their vertical and horizontal positions are largely identical, however, GIF22 and GIF25 are significantly older than the associated samples (Fig. 5). Since the dosimetry and dating of GIF22 and GIF25 are not in question, the only possible explanation for the apparent discrepancy is that flints burned during earlier occupations, potentially those represented by Layers 9 and 10, were introduced into Layer 7 via bioturbation, erosion, or human agency.

The 1997–2001 excavations at Ortvale Klde were conducted in the southern chamber of the rockshelter in units where Layers 9 and 10 are not encountered (Fig. 1). Samples from these layers were selected for dating from extant collections curated in the Georgian State Museum (Layer 9: $n = 10$; Layer 10: $n = 11$). These specimens were excavated during the campaigns of D. Tushabramishvili in the late 1970s and early 1980s. TL was successfully applied to 33.3% of these specimens and indicates statistically identical ages for Layer 9 (50.1 ka BP_{TL}) and Layer 10 (51.3 ka BP_{TL}; Fig. 5). In total these specimens produce a coherent sequence of dates that increase in age with depth. Among the TL results for Ortvale Klde, the main point of departure is the early date associated with Layer 4c. At present this deviation cannot be explained.

ESR analysis

ESR dating was performed on the enamel of six ungulate (*Capra caucasica*) teeth collected from Layer 7 during the 1999 excavation, of which five specimens (83.3%) provided results. All specimens were retrieved within 5–30 cm (horizontal: x and y) and 8–12 cm (vertical: z) of one of two dosimeters inserted into the unexcavated section the previous season. Samples OK2 and OK3 are derived from two distinct elevations in Unit E8a, while OK4–OK6 are derived from the same elevation (403–404 cm) within Unit E9c (Fig. 1). Two specimens, OK5 and OK6, represent individual teeth derived from an articulated tooth row.

Sample preparation and pretreatment

The enamel on all teeth was in excellent condition with a pristine white color. The teeth were prepared according to a published protocol (Rink et al., 1994) and the sediments surrounding the teeth were analyzed for their Uranium (U), Thorium (Th), and Potassium (K) concentrations, and were used to determine the β and γ dose rates to the enamel from sediment. The gamma plus cosmic dose rate was determined in-situ using thermoluminescence dosimeters. Ages were calculated using the software ROSY version 1.41 (Brennan et al., 1997). Since there has been very little uranium uptake at the site and the cosmic dose rate is very low, there is little statistical difference between the EU and LU ages. Under such conditions, ages then become more dependent upon the moisture content of the sediments, which can strongly affect beta and

Table 2
TL Dating Results for Ortvale Klde[a]

							DOSES (μGy/a)											ED		Age	
GIF#	L.	Unit	Elevation	U ppm	Th ppm	K %	S-α (/10^3α/ cm^2)	α	β	Internal	±	Gamma	±	External	±	Annual	±	Gy	±	ka	±
115	4c	G7c	286–291	1.27	0.07	0.06	19.3	414	231	654	48	223	150	373	43	1026	64	29.7	0.5	28.9	2.6
108	4c	G7a	286–291	3.34	0.14	0.07	35.2	1979	545	2552	309	212	150	362	42	2914	317	81.7	2.1	28.0	4.5
116	4c	G7c	286–292	0.82	0.18	0.07	20.4	298	176	482	34	218	150	368	42	850	54	25.6	0.5	30.1	2.6
114	4c	G7c	291–300	1.44	0.12	0.07	18.8	461	269	743	55	218	150	368	42	1111	69	30.9	0.8	27.8	2.5
106	4c	G7a	300–304/307	6.90	0.16	0.06	23.2	2680	1056	3776	314	217	150	367	43	4143	317	123.4	3.6	29.8	3.6
119	5	G7a	304/307–315	0.11	0.09	0.06	11.7	26	62	90	5	204	150	354	43	444	43	18.8	0.7	42.3	4.7
118	5	G7a	315–321	0.93	0.08	0.05	16.6	263	178	449	31	200	150	350	42	799	52	41.4	1.7	51.8	4.7
5	5	F8a	321–333	1.01	0.06	0.04	14.4	246	184	436	39	242	150	392	43	828	58	42.4	0.6	51.2	4.8
121	5	G8c	326–331	0.70	0.07	0.04	26.1	312	133	450	36	221	150	371	42	820	55	33.6	0.8	41.0	3.7
9	6	E9c	344–352	0.99	0.11	0.05	17.0	290	188	484	35	397	150	547	51	1031	62	50.6	1.9	49.0	4.0
10	6	E9c	344–352	0.50	0.05	0.03	6.9	59	98	160	10	401	150	551	52	711	53	37.7	1.1	53.0	4.6
12	6	E9a	348	1.47	0.06	0.05	32.3	799	254	1060	108	401	150	551	52	1611	120	59.0	0.8	36.6	4.0
15	6	E9a	348	1.00	0.06	0.06	9.4	159	193	362	23	389	150	539	50	900	55	41.0	0.7	45.6	3.5
20	7	E8d	385/392–392	1.45	0.06	0.04	25.7	627	247	882	90	314	150	464	43	1346	100	55.3	1.1	41.1	4.5
22	7	E8d	385/392–392	3.43	0.19	0.05	12.0	697	548	1262	134	316	150	466	43	1727	140	104.6	2.5	60.5	7.4
28	7	E8b	386–392	2.95	0.16	0.06	21.7	1083	481	1579	127	316	150	466	43	2044	134	84.3	1.2	41.2	4.2
30	7	E8b	386–392	2.32	0.14	0.05	28.3	1110	381	1507	132	311	150	461	42	1968	138	82.3	1.1	41.8	4.5
31	7	E8b	386–392	3.46	0.17	0.05	24.2	1412	548	1976	164	316	150	466	43	2442	169	100.9	3.0	41.3	4.5
32	7	E8b	386–392	1.10	0.07	0.06	19.7	367	206	583	45	306	150	456	42	1039	62	46.6	1.2	44.9	3.8
24	7	E8a	387–392	0.36	0.08	0.05	16.2	103	90	197	13	309	150	459	42	656	44	29.1	0.4	44.3	3.5
25	7	E8a	387–392	1.87	0.05	0.05	13.4	420	310	741	54	313	150	463	43	1204	69	91.3	3.1	75.9	6.5
26	7	E8a	387–392	1.63	0.06	0.04	15.6	426	273	708	73	314	150	464	43	1172	85	56.9	1.2	48.6	5.1
122	9	GSM	79:118†	1.43	0.07	0.05	22.0	530	250	790	77	207	150	357	42	1147	88	53.3	0.7	46.4	5.1
131	9	GSM	81:383†	2.37	0.14	0.05	19.3	774	388	1182	103	205	150	355	42	1537	112	85.2	1.6	55.4	6.1
132	10	GSM	80:470†	2.01	0.04	0.05	28.5	958	331	1304	126	207	150	357	42	1661	132	91.2	3.5	54.9	6.6
134	10	GSM	81:434†	1.90	0.06	0.04	15.5	493	309	816	66	207	150	357	42	1173	78	54.2	0.9	46.2	4.5
136	10	GSM	81:436†	1.44	0.08	0.05	19.7	479	251	741	70	207	150	357	42	1098	82	55.7	1.6	50.7	5.5
137	10	GSM	81:524†	0.78	0.08	0.03	17.7	236	142	389	63	196	150	346	40	735	74	38.5	0.7	52.4	7.3
141	10	GSM	81:677†	0.82	0.08	0.03	18.5	259	148	414	58	206	150	356	42	769.4	71.4	47.7	1.0	62.0	7.9

[a] GIF# 12, 22, 25 have been omitted from further analysis. Layers 9 and 10 were not re-excavated during this project but datable specimens were selected from the collections of the Georgian State Museum (GSM) and are reported here with their respective internal inventory number (†). The internal (alpha + beta) dose-rate was deduced from the radioisotopic contents (U, Th, K) of the dated specimen and from specific annual dose-rates given by Adamiec & Aitken (1998). It also takes account of the S-alpha parameter that is a measure of the efficiency of the α relative to β particles to produce a TL signal (Valladas and Valladas, 1982). The external dose-rate was deduced from measurements taken in the field by dosimeters and includes a cosmic contribution of 150 μGy/a. The equivalent dose (ED) is an estimate of the dose accumulated by a specimen since its last heating in a fireplace. It was determined by measuring the natural TL emission around 380 °C and by calibrating it using artificial radiation sources (Mercier et al., 1992). The final uncertainties associated with the TL ages include both statistical and systematic errors, given at 68% confidence level. Please see Figs. 1 and 4 for sample locations.

Table 3
Weighted Means of TL Results from Ortvale Klde[a]

GIF#	Layer	Unit	Elevation	Age BP ± 1σ	t-value	Weighted Mean
115	4c	G7c	286–291	28900 ± 2600	0.02	28946 ± 1310
108	4c	G7a	286–291	28000 ± 4500	0.20	
116	4c	G7c	286–292	30100 ± 2600	0.40	
114	4c	G7c	291–300	27800 ± 2500	0.41	
106	4c	G7a	300–304/307	29800 ± 3600	0.22	
119	5	G7a	304/307–315	42300 ± 4700	0.67	45785 ± 2198
118	5	G7a	315–321	51800 ± 4700	1.16	
5	5	F8a	321–333	51200 ± 4800	1.03	
121	5	G8c	326–331	41000 ± 3700	1.11	
9	6	E9c	344–352	49000 ± 4000	0.10	48538 ± 2286
10	6	E9c	344–352	53000 ± 4600	0.87	
15	6	E9a	348	45600 ± 3500	0.70	
20	7	E8d	385/392–392	41100 ± 4500	0.46	43289 ± 1593
28	7	E8b	386–392	41200 ± 4200	0.47	
30	7	E8b	386–392	41800 ± 4500	0.31	
31	7	E8b	386–392	41300 ± 4500	0.42	
32	7	E8b	386–392	44900 ± 3800	0.39	
24	7	E8a	387–392	44300 ± 3500	0.26	
26	7	E8a	387–392	48600 ± 5100	0.99	
122	9	GSM	79:118†	46400 ± 5100	0.58	50103 ± 3913
131	9	GSM	81:383†	55400 ± 6100	0.73	
132	10	GSM	80:470†	54900 ± 6600	0.50	51322 ± 2671
134	10	GSM	81:434†	46200 ± 4500	0.98	
136	10	GSM	81:436†	50700 ± 5500	0.10	
137	10	GSM	81:524†	52400 ± 7300	0.14	
141	10	GSM	81:677†	62000 ± 7900	1.28	

[a] † = Layers 9 and 10 were not re-excavated during this project but datable specimens were selected from the collections of the Georgian State Museum (GSM) and are reported here with their respective internal inventory number. Please see Figs. 1 and 4 for sample locations.

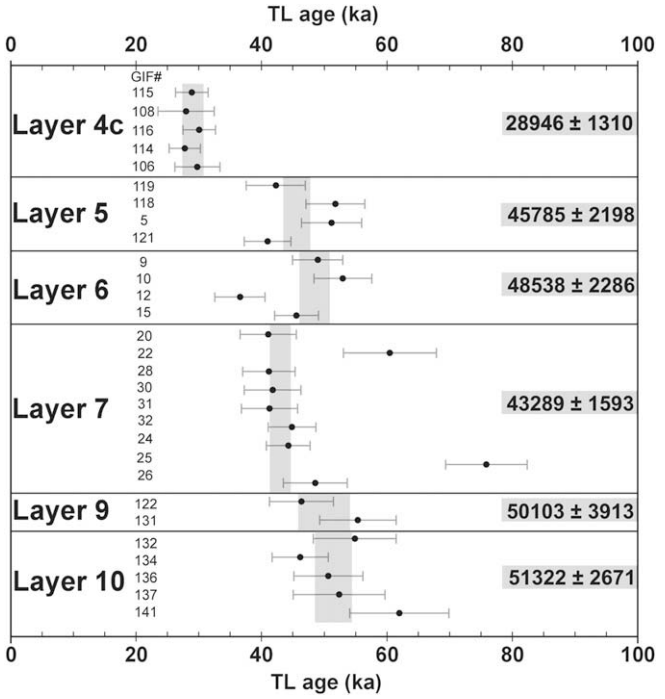

Fig. 5. TL data arranged by layer. All measurements are plotted with 1σ. Vertical gray bars indicate the weighted mean of several determinations within the same geological layer that are statistically identical at 2σ.

gamma dose-rates. Table 4 presents the technical data for the five dated samples from Layer 7. Further data and the age estimates for each specimen are provided in Table 5; Table 6 presents the weighted means.

Based on the discard protocol outlined above, only one ESR specimen was omitted from analysis; OK2, located approximately 25 cm higher than the nearest specimen, is much older than the underlying samples (*t*-value >2). Of the remaining specimens, a weighted mean of 44.5 ka BP_{ESR} was attained following the early uptake model while the linear uptake model produced a result of 47.9 ka BP_{ESR} (Fig. 6). Both model results are statistically identical at 1 sigma, and both are in general agreement with the TL results from Layer 6 and Layer 7 (Fig. 5 and 6).

Radiocarbon analysis

A total of 103 specimens were submitted to the radiocarbon dating laboratory at the Weizmann Institute of Science and the NSF Facility in Arizona for dating via the AMS technique. Twenty-eight (52.8%) of the 53 submitted charcoal samples produced results, while 14 (28%) of 50 bone samples (*Bison priscus* and *Capra caucasica*) could be dated. The stratigraphic contexts, technical data, and ages associated with these samples are summarized in Table 7. The in-lab selection of bone and charcoal samples for AMS dating followed a strict analysis and prioritization scheme (see below) with the actual dating performed only on samples that provided high quality datable material. In general, samples were selected for analysis based on their size (larger pieces of charcoal; thick bones); the Fourier transform infrared (FTIR) spectrum of charcoal, mineral, and organic bone fraction; and C%. Specifically, bone samples were screened via FTIR for the quality of their inorganic fraction and their acid insoluble fraction (collagen), with rough quantification of the collagen content (Yizhaq et al., 2005). Prior to oxidation to CO_2, selected collagen samples were analyzed again with FTIR to assess their purity and the presence/absence of other minerals (e.g., clay). Charcoal samples were screened for their quality through FTIR, their recovered mass, and C%. Prior to oxidation and graphitization, charcoal samples were again checked for purity and, regardless of the recovered mass, were processed for measurement. As with bone samples, pre-treated charcoal samples at this stage were excluded from further analysis if they did not produce a clean FTIR spectrum (e.g., clay presence; Yizhaq et al., 2005). Several samples that did not pass this strict quality assessment (see below) were nonetheless submitted for dating in order to

Table 4
Technical data on ESR Samples from Layer 7 at Ortvale Klde[a]

S#	Unit	Elevation	D_E (Gy)	U En (ppm)	U Den (ppm)	U Sed (ppm)	K Sed (wt %)	Th Sed (ppm)	Enamel Thickness (μm)	Sed Side Rem (μm)	Den Side Rem (μm)
OK2	E8a	376	42.89 ± 1.80	<0.1	4.60	1.79	1.23 ± 0.05	4.14 ± 0.23	863 ± 142	88 ± 44	97 ± 49
OK3	E8a	401	29.17 ± 0.68	<0.1	6.40	2.00	1.18 ± 0.05	4.53 ± 0.23	1313 ± 72	86 ± 43	92 ± 46
OK4	E9c	403	51.20 ± 1.25	<0.1	10.42	2.46	1.83 ± 0.08	6.45 ± 0.25	600 ± 42	47 ± 24	50 ± 25
OK5	E9c	404	45.94 ± 1.38	<0.1	7.62	4.34	1.39 ± 0.06	4.68 ± 0.26	612 ± 103	75 ± 49	73 ± 47
OK6	E9c	404	43.84 ± 1.34	0.43	6.83	4.31	1.38 ± 0.06	4.84 ± 0.28	652 ± 140	42 ± 21	76 ± 38

[a] Abbreviations: D_E is equivalent dose, U is uranium, K is potassium, Th is thorium, Sed is sediment, Den is dentine, Rem is removed, ppm is parts per million, wt % is weight percent, Gy is Gray, μm is micrometer. NA is not applicable. Errors in Th and K values range from ±2–8% of the value and are not reported here. Errors in U values are ±0.1 ppm. ^{238}U concentrations in enamel and dentine and sediment were determined using delayed neutron counting, while ^{232}Th and ^{40}K in sediment were determined using instrumental neutron activation analysis at the McMaster Nuclear Reactor. Samples OK5 and OK6 derive from the same tooth row. Please see Fig. 1 for sample locations.

Table 5
ESR Dating Results for Layer 7 at Ortvale Klde[a]

					Early Uptake				Linear Uptake					
S#	Unit	z	Gamma Plus Cosmic Dose Rate (μ Gy/a)	EU, LUβ Sed Dose Rate (μGy/a)	α En Dose Rate (μGy/a)	β En Dose Rate (μGy/a)	β Den Dose Rate (μGy/a)	Total Dose Rate (μGy/a)	α En Dose Rate (μGy/a)	β En Dose Rate (μGy/a)	β Den Dose Rate (μGy/a)	Total Dose Rate (μGy/a)	EU Age BP	LU Age BP
OK2	E8a	376	478 ± 48	181.3	0	0	59.3	718.6	0	0	27.8	687.2	59700 ± 5800	62400 ± 6200
OK3	E8a	401	478 ± 48	121.5	0	0	56.1	655.6	0	0	26.7	626.2	44500 ± 3600	46600 ± 4000
OK4	E9c	403	554 ± 55	369.5	0	0	168.6	1092.1	0	0	79.7	1003.17	46900 ± 3200	51000 ± 3800
OK5	E9c	404	554 ± 55	331.5	0	0	120.4	1005.9	0	0	56.9	942.3	45700 ± 4100	48800 ± 4600
OK6	E9c	404	554 ± 55	338.7	74.1	18.5	97.8	1083.0	32.7	8.5	46.7	980.5	40500 ± 3600	44700 ± 4200

[a] OK2 has been omitted from further analysis. Abbreviations: EU is early uptake model; LU is linear uptake model; β is beta; α is alpha; Cem is cementum; Den is dentine; En is enamel. The moisture content assumed for the beta dose calculations was 10 ± 10%, while the gamma plus cosmic dose rates were determined using thermoluminescence capsules which measured these dose rates in-situ. The use of these dose rates assumes that the in-situ moisture content at the time of measurement was similar to the average moisture content during the burial period. General preparation procedures of the teeth for ESR dating followed the protocol outlined in Rink et al. (1994). ESR measurements were carried out using a JEOL JES-FA100 X-band spectrometer at power 2.0 mW, modulation amplitude 0.5 mT, centre field 336.0 mT, width 5.0 mT, scan rate 0.167 mT/sec, time constant 0.1 sec. Due to the relatively small equivalent doses, linear fits were used to establish the D_E from the dose response data. Ages were calculated using the software ROSY version 2.0, which is a windows version of ROSY version 1.41 Brennan et al. (1997), and which utilizes one-group theory for beta particle transport. Samples OK5 and OK6 derive from the same tooth row. Please see Fig. 1 for sample locations.

Table 6
Weighted Means of ESR Results from Layer 7 at Ortvale Klde[a]

S#	Unit	Elevation	EU Age BP	t-value	EU Weighted Mean	LU Age BP	t-value	LU Weighted Mean
OK3	E8a	401	44500 ± 3600	0.00	44491 ± 1792	46600 ± 4000	0.28	47877 ± 2060
OK4	E9c	403	46900 ± 3200	0.66		51000 ± 3800	0.72	
OK5	E9c	404	45700 ± 4100	0.27		48800 ± 4600	0.18	
OK6	E9c	404	40500 ± 3600	0.99		44700 ± 4200	0.68	

[a] Sample OK2 was omitted from this analysis. Samples OK5 and OK6 derive from the same tooth row. Please see Fig. 1 for sample locations.

verify the type of contamination and chronometric "noise" that would be introduced were these quality control measures not implemented.

Sample preparation and pretreatment

The charcoal and bone samples submitted to the Weizmann Institute of Science were pre-treated to remove possible environmental contaminants (Yizhaq et al., 2005). Pretreatment included the removal of humic material, a common source of contamination, from all charcoal and bone specimens. FTIR analysis was performed on the collagen material extracted from each bone sample to screen the quality before oxidation, graphitization, and AMS measurement. Dating was performed only on samples that produced an infrared spectra similar to collagen from modern bone. This spectrum is characterized by a strong peak at 1,454 cm-1 due to the amino acid proline, together with the amide I and amide II absorptions at about 1,650 and 1,540 cm-1, respectively. In order to verify the effectiveness of pre-screening based on FTIR analysis, three samples were radiocarbon dated although they did not pass the quality test. These samples (RTA 3425, RTA 3427, RTA 3428) had an infrared spectrum showing a strong presence of clay minerals in the gelatin (clay carries carbon and can therefore affect the age). The bone pre-treatment procedure was not able to separate the clay from the gelatin fraction. The ^{14}C ages are in each case significantly younger than the ages of the samples from the same layer. This might indicate the existence of a young source for the organic material in the clay. If this is due to the presence of young humic substances dissolved in the water, then this hypothesis could also explain the young ages of two charcoal samples, which were dated as test cases. Sample RTT 4206, due to its very small size, was not pre-treated for humic substances, and for sample RTT 3965, the weight loss during pre-treatment was 80%. In the first case it shows that the humic substances are younger, and in the second case, the sample was very degraded and may have been exposed to the humic substances in a more substantial way. As indicated in Table 7, all five of these samples are omitted from further analysis. Samples RTT 3826a and RTT 3826b represent a single bone that was divided into two equal portions, one of which was pretreated at the radiocarbon laboratory in Oxford (3826a) and the other at the Weizmann Institute of Science (3826b), with both samples dated in Arizona. A total of four charcoal samples were divided into equal portions and submitted to the Weizmann Institute of Science (RTT 4207, 4208, 4214, 4212) and Arizona (AA 45862, 45863, 45865, 45864) for pretreatment and dating (Table 7). Table 8 presents weighted means for the uncalibrated and calibrated data and Table 9 presents an analysis of the split samples. Fig. 7 presents all AMS samples arranged according to depth and material.

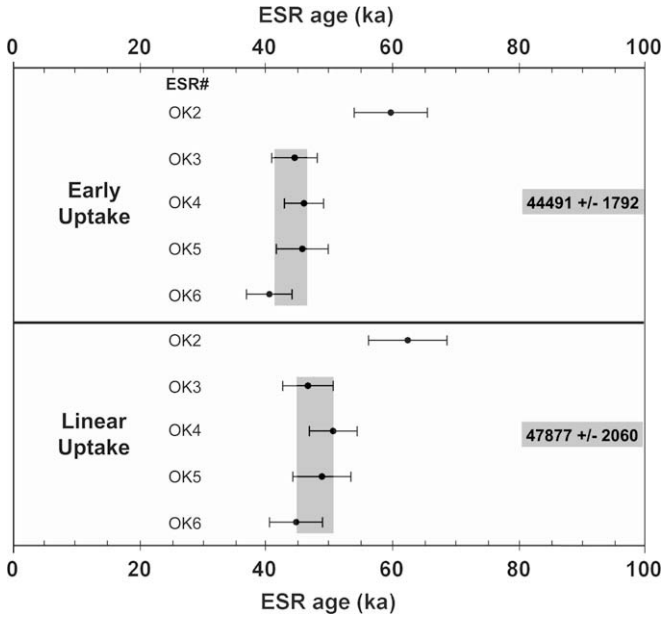

Fig. 6. ESR data arranged by layer. All measurements are plotted with 1σ. Vertical gray bars indicate the weighted mean of several determinations within the same geological layer that are statistically identical at 2σ.

Table 7
AMS Data for Ortvale Klde[a]

Lab#	Layer	Material	Unit	Elevation	$\delta^{13}C$ ‰ PDB	^{14}C Age BP ± 1σ	Age CalBP ± 1σ	Discard:Criteria
RTT 3824	2	Bone	G6a	230–243/246	−19.15	21170 ± 140	25329 ± 363	No
RTT 4206	2	Bone	G6d	230	too small	18080 ± 115	21820 ± 368	Yes: Not cleaned for humic
AA 38195	3	Charcoal	G8a	236	−19.30	21580 ± 230	25799 ± 534	No
AA 38196	3	Charcoal	G8a	238	−21.10	21740 ± 220	25987 ± 583	No
RTT 3964	4b	Charcoal	G8a	263	−25.04	27000 ± 260	31742 ± 201	No
RTT 3825	4b	Bone	G7c	261/265–272	−18.98	23770 ± 200	28694 ± 421	No
RTT 4724	4b	Bone	G7d	268–282	−19.90	32960 ± 550	37453 ± 886	Yes: <Accuracy, <Context
AA 38193	4c	Charcoal	E9d	276	−26.60	30660 ± 430	34889 ± 451	No
AA 38197	4c	Charcoal	F8c	285	−25.60	30260 ± 490	34520 ± 444	No
AA 45862	4c	Charcoal	G8d	286	−25.10	28840 ± 350	33308 ± 473	Yes: <Accuracy
RTT 4207	4c	Charcoal	G8d	286	−25.10	31900 ± 780	36380 ± 1205	No
AA 45863	4c	Charcoal	G8b	287	−26.00	29950 ± 410	34140 ± 355	Yes: <Accuracy
RTT 4208	4c	Charcoal	G8b	287	−26.10	32200 ± 550	36701 ± 982	No
RTT 4209	4c	Charcoal	G8b	287	−25.70	31800 ± 400	35825 ± 632	No
RTT 4210	4c	Charcoal	G8b	287	−25.80	31700 ± 500	35785 ± 723	No
RTT 3965	4c	Charcoal	G7c	289	−24.82	26890 ± 280	31610 ± 267	Yes: Large loss of material
RTT 4211	4c	Charcoal	G6d	296	−24.90	32300 ± 550	36809 ± 966	No
AA 45865	4c	Charcoal	G8d	298	−23.70	32510 ± 530	37020 ± 897	No
RTT 4214	4c	Charcoal	G8d	298	−23.70	34100 ± 800	39146 ± 1340	No
RTT 4213	4c	Charcoal	G7d	298	−23.80	34600 ± 600	39781 ± 911	No
AA 45864	4c	Charcoal	G6d	300	−25.10	33700 ± 620	38861 ± 1506	No
RTT 4212	4c	Charcoal	G6d	300	−25.00	34300 ± 650	39560 ± 999	No
RTT 4725	4d	Bone	G8d	292/298–308	−19.30	38100 ± 935	42714 ± 805	No
RTT 4726	4d	Bone	G8d	292/298–308	−18.70	32620 ± 520	37126 ± 864	Yes: <Accuracy, <Context
RTT 4727	4d	Bone	G7b	296/299–309	−19.45	45790 ± 2435	49770 ± 3180	Yes: <Accuracy, <Context
RTT 3826b	5	Bone	G7a	304/307–315	−18.77	37770 ± 1000	42446 ± 783	No
RTT 3826a	5	Bone	G7a	304/307–316	−18.77	39280 ± 1200	43396 ± 890	No
RTA 3427	5	Bone	E8a	312–317	−20.40	22860 ± 190	27490 ± 430	Yes: Clay in collagen following pretreatment
RTA 3426	5	Bone	E8c	331–333/339	−19.40	34900 ± 700	39926 ± 965	Yes: <Accuracy, <Context
RTT 4215	6	Charcoal	G8b	335	−22.90	>45000	>45000	Yes: No Precision
RTT 4216	6	Charcoal	G8d	350	−24.10	46600 ± 2700	50833 ± 3672	No
RTT 3961	6	Charcoal	F8a	355	−25.48	42920 ± 1880	46730 ± 2053	No
RTT 4217	6	Charcoal	G8b	360	−25.30	48400 ± 3500	53721 ± 5221	No
AA 38194	6	Charcoal	E8c	361	−24.00	31820 ± 890	36353 ± 1279	Yes: <Accuracy, <Context
AA 45866	6	Charcoal	G8b	363	−24.40	46400 ± 2600	50541 ± 3510	No
RTT 4219	6	Charcoal	G8b	363	−24.30	40900 ± 1500	44605 ± 1360	No
RTT 3962	6	Charcoal	E8b	365	−25.45	41100 ± 1500	44773 ± 1410	No
RTA 3425	6	Bone	F8a	345–350	−18.90	25400 ± 300	30333 ± 429	Yes: Clay in collagen following pretreatment
AA 45867	7	Charcoal	G7b	377	−22.20	47600 ± 3200	52369 ± 4521	Yes: <Accuracy, <Context
RTT 4220	7	Charcoal	G7b	377	−22.80	>45000	>45000	Yes: No Precision
RTA 3430	7	Bone	E9a	382–387	−19.50	43000 ± 1150	46962 ± 1820	No
RTA 3428	7	Bone	E8a	392–397	−17.50	40800 ± 1250	44424 ± 1139	Yes: Clay in collagen following pretreatment

[a] Abbreviations: RTA and RTT = Weizmann Institute of Science; AA = National Science Foundation Arizona AMS Laboratory. Italicized samples blocked together represent a single charcoal specimen that was split into equal halves and dated by two independent labs. Please see Figures 1 and 4 for sample locations. Data calibrated with CalPal-online (Danzeglocke, U., Jöris, O., Weninger, B., 2007. CalPal-2007online. http://www.calpal-online.de/).

The EUP deposits

A single bone date from Layer 2 and two charcoal dates from Layer 3 suggest ages of 21,170 ± 140 ^{14}C BP and 21,664 ± 159 ^{14}C BP, respectively. While it was not possible to date any specimens from Layer 4a, thus leaving a significant stratigraphic gap (~25 cm) in our data, single bone and charcoal dates were determined for Layer 4b. These estimates, derived from different materials, overlap only at 7 standard deviations. Without any other chronometric point of reference it is not possible to estimate the age of Layer 4b other than to say it lies somewhere between that determined for Layer 3 and Layer 4c. In Layer 4c, we attained 12 charcoal dates that cluster into three statistically independent chronometric groups that increase in age with depth. Two samples (AA 45862, AA 45863) are omitted from the analysis as they do not conform in age to stratigraphically associated samples (Table 7; Fig. 7), and do not overlap at 2-sigma with their split partners (Table 9; Fig. 7). The weighted mean for the youngest group ($n = 2$) is 30,486 ± 323 ^{14}C BP, that of the middle group ($n = 6$) is 32,039 ± 213 ^{14}C BP, and that of the oldest group ($n = 4$) is 34,188 ± 328 ^{14}C BP (Fig. 7). Layer 4d, the earliest EUP occupation at Ortvale Klde, produced three divergent bone dates. We omit two samples (RTT 4727 and RTT 4726) from further analysis as one is considerably younger and the other considerably older than the age determinations for Layer 4c (Fig. 7). Consequently, we are left with a single bone date of 38,100 ± 935 ^{14}C BP for Layer 4d. While this estimate is in stratigraphic accord with the overlying data for Layer 4c, it is a single estimate and must be treated with caution. Without further data from Layer 4d, our conservative estimate for the First Appearance Date (FAD) of the EUP at Ortvale Klde is some time between 38,100 ± 935 ^{14}C BP (Layer 4d) and 34,188 ± 328 ^{14}C BP (Layer 4c; Fig. 7).

The LMP deposits

The LMP at Ortvale Klde ends with Layer 5, which at present is dated by a single bone (RTT 3826) that was split into two segments (RTT 3826a and RTT 3826b). Each segment was independently pretreated in two labs, and each was subsequently dated in Arizona (Fig. 7). This procedure yielded two statistically identical dates with a weighted mean of 38,389 ± 768 ^{14}C BP. In the context of the shift from the Middle to the Upper Paleolithic, the data from Layer 4d and Layer 5 could be taken to indicate either the rapid replacement of Neandertals by modern humans at ~38 ka ^{14}C BP or a lengthier process that spanned ~38–34 ka ^{14}C BP (Fig. 7). The current chronometric resolution available from these two layers is not suitable to resolve this issue and so we prefer the conservative estimate of ~38–34 ka ^{14}C BP for the replacement and the Last Appearance Date (LAD) of the Neandertals (Fig. 7). The stratigraphic

Table 8
Weighted Means for Raw and Calibrated AMS data from Ortvale Klde[a]

Lab#	Layer	Material	^{14}C Age BP ± 1σ	t-value	Weighted Mean	Age Cal BP$_{Hulu}$ ± 1σ	t-value	Weighted Mean
RTT 3824	2	Bone	21170 ± 140	0.00	21170 ± 140	25329 ± 363	0.00	25329 ± 363
AA 38195	3	Charcoal	21580 ± 230	0.30	21664 ± 159	25799 ± 534	0.13	25885 ± 394
AA 38196	3	Charcoal	21740 ± 220	0.28		25987 ± 583	0.15	
RTT 3964	4b	Charcoal	27000 ± 260	0.00	27000 ± 260	31742 ± 201	0.00	31742 ± 201
RTT 3825	4b	Bone	23770 ± 200	0.00	23770 ± 200	28694 ± 421	0.00	28694 ± 421
AA 38193	4c	Charcoal	30660 ± 430	0.32	30486 ± 323	34889 ± 451	0.34	34704 ± 316
AA 38197	4c	Charcoal	30260 ± 490	0.38		34520 ± 444	0.33	
RTT 4207	4c	Charcoal	31900 ± 780	0.17	32039 ± 213	36380 ± 1205	0.09	36269 ± 344
RTT 4210	4c	Charcoal	31700 ± 500	0.62		35785 ± 723	0.60	
RTT 4209	4c	Charcoal	31800 ± 400	0.53		35825 ± 632	0.62	
RTT 4208	4c	Charcoal	32200 ± 550	0.27		36701 ± 982	0.42	
RTT 4211	4c	Charcoal	32300 ± 550	0.44		36809 ± 966	0.53	
AA 45865	4c	Charcoal	32510 ± 530	0.83		37020 ± 897	0.78	
RTT 4214	4c	Charcoal	34100 ± 800	0.10	34188 ± 328	39146 ± 1340	0.23	39475 ± 559
RTT 4213	4c	Charcoal	34600 ± 600	0.60		39781 ± 911	0.29	
AA 45864	4c	Charcoal	33700 ± 620	0.70		38861 ± 1506	0.38	
RTT 4212	4c	Charcoal	34300 ± 650	0.15		39560 ± 999	0.07	
RTT 4725	4d	Bone	38100 ± 935	0.00	38100 ± 935	42714 ± 805	0.00	42714 ± 805
RTT 3826b	5	Bone	37770 ± 1000	0.49	38389 ± 768	42446 ± 783	0.42	42860 ± 588
RTT 3826a	5	Bone	39280 ± 1200	0.63		43396 ± 890	0.50	
RTT 4216	6	Charcoal	46600 ± 2700	1.36	42764 ± 806	50833 ± 3672	1.32	45872 ± 824
RTT 3961	6	Charcoal	42920 ± 1880	0.08		46730 ± 2053	0.39	
RTT 4217	6	Charcoal	48400 ± 3500	1.57		53721 ± 5221	1.48	
AA 45866	6	Charcoal	46400 ± 2600	1.34		50541 ± 3510	1.29	
RTT 4219	6	Charcoal	40900 ± 1500	1.09		44605 ± 1360	0.80	
RTT 3962	6	Charcoal	41100 ± 1500	0.98		44773 ± 1410	0.67	
RTT 3430	7	Bone	43000 ± 1150	0.00	43000 ± 1150	46727 ± 1818	0.00	46727 ± 1818

[a] Data calibrated with CalPal-online (Danzeglocke, U., Jöris, O., Weninger, B., 2007. CalPal-2007online. http://www.calpal-online.de/). Note that AA 45865 and RTT 4214 represent a single split sample but are analyzed separately. Please see Figs. 1 and 4 for sample locations.

break between the LMP and EUP is clear and there is no interstratification between these two entities.

Three AMS estimates from Layer 6 were omitted from this analysis due to their young age (AA 38194), poor collagen quality (RTT 3425), or minimum age estimate (RTT 4215). The remaining six results provide a weighted mean of 42,764 ± 806 ^{14}C BP (Fig. 7). Two charcoal specimens were omitted from the analysis of Layer 7 due to their minimum age estimate (RTT 4220) or excessive age (AA 45967), and one bone specimen (RTA 3428) was omitted as it contained clay following pretreatment. The remaining bone specimen produced an age of 43,000 ± 1,150 ^{14}C BP that is statistically identical to that produced for Layer 6. These results are also in accord with the associated TL estimates reported above. Based on the AMS determinations, Layers 6 and 7 are statistically identical and cannot be separated. Since the stratigraphic boundary between these two archaeological layers is not as distinct as those between younger layers, and signs of bioturbation are readily observable, this statistical similarity in age is not surprising. Although on stratigraphic grounds Layer 6 should be younger than Layer 7, we interpret this close age relationship as the result of rapid, mostly anthropogenic deposition, perhaps in association with repeated and lengthy occupations of the site, accompanied by post-depositional taphonomic forces.

Calibration

While the ability to estimate the radiocarbon calibration curve beyond 26 ka cal BP has been called into question by members of the IntCal group for a variety of commonly cited reasons (e.g., Bronk Ramsey et al., 2006 and citations therein), others (e.g., van Andel and Davies, 2003; van Andel, 2005; Weninger and Jöris, this issue) argue for a stratigraphic path to calibration beyond 26 ka cal BP. In this paper we calibrate the AMS results using the Cologne

Table 9
Split AMS samples from Ortvale Klde[a]

Lab#	Layer	Material	δ^{13}C ‰ PDB	^{14}C Age BP ± 1σ	t-value	Weighted Mean	Age Cal BP$_{Hulu}$ ± 1σ	t-value	Weighted Mean
RTT 4207	4c	Charcoal	−25.10	31900 ± 780	*3.02*	29353 ± 319	36380 ± 1205	*2.07*	33718 ± 440
AA 45862	4c	Charcoal	−25.10	28840 ± 350	1.08		33308 ± 473	0.63	
RTT 4208	4c	Charcoal	−26.10	32200 ± 550	*2.26*	30754 ± 329	36701 ± 982	*2.18*	34436 ± 334
AA 45863	4c	Charcoal	−26.00	29950 ± 410	1.53		34140 ± 355	0.61	
RTT 4212	4c	Charcoal	−25.00	34300 ± 650	0.40	33986 ± 449	39560 ± 999	0.16	39346 ± 832
AA 45864	4c	Charcoal	−25.10	33700 ± 620	0.37		38861 ± 1506	0.28	
RTT 4214	4c	Charcoal	−23.70	34100 ± 800	1.21	32995 ± 442	39146 ± 1340	0.96	37678 ± 745
AA 45865	4c	Charcoal	−23.70	32510 ± 530	0.70		37020 ± 897	0.56	
RTT 3826b	5	Bone	−18.77	37770 ± 1000	0.49	38387 ± 768	42446 ± 783	0.42	42860 ± 588
RTT 3826a	5	Bone	−18.77	39275 ± 1200	0.62		43396 ± 890	0.50	

[a] Italicized t-values denote samples that fall outside the 2 sigma-level of standard deviation for the weighted mean. Note that in the first two reported cases the split samples are statistically divergent. See Table 7 for sample context and properties.

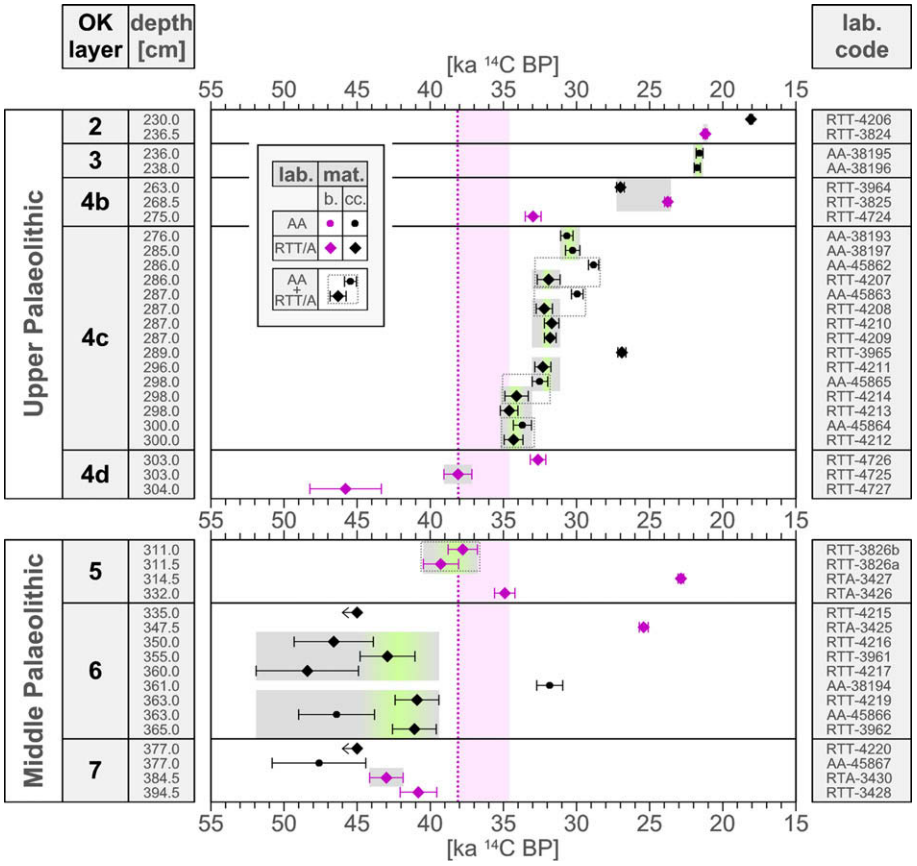

Fig. 7. Age-depth graph of Ortvale Klde with radiocarbon results (ka ^{14}C BP) plotted against stratigraphy. Dated samples are distinguished by material (mat.), separating bone (b.) and charcoal (cc.), and by laboratory (lab.), with "AA" representing the NSF-Arizona AMS Laboratory (USA), and "RTT" and "RTA" the Weizmann Institute of Science (Israel). All measurements are plotted with 1σ while determinations of infinite age are indicated by an arrow. Horizontal gray bars indicate the most likely age estimates based on stratigraphic position and age overlap. Green shading indicates the weighted mean of several determinations within the same geological layer that are statistically identical at 2σ. The five boxes with grey dotted lines (Layer 5: n=1; Layer 4d: n=4) denote five individual samples split between the NSF-Arizona AMS Laboratory and the Weizmann Institute of Science. The pink dotted line indicates the oldest possible estimate for the Middle to Upper Paleolithic boundary at Ortvale Klde (~38.0 ka ^{14}C BP), while the vertical pink bar indicates the age range during which this "transition" can be dated (~38.0 and ~34.5 ka ^{14}C BP). This age range is determined based on several criteria including the precise stratigraphic position of each sample and the dates from Layers 5 and 4d.

Radiocarbon Calibration and Paleoclimatic Research Package (CALPAL: CalCurve: CalPal-2007$_{Hulu}$). This program performs automatic calendric age-conversions of ^{14}C and AMS data from dates expressed as Uncal BP to dates expressed as Cal BC and Cal BP$_{Hulu}$. It also takes into consideration fluctuations in atmospheric carbon isotope production. The importance of the CALPAL program, beyond its ability to provide calendric age-conversions of dates, lies in the fact that ^{14}C or AMS data thus modified can be compared directly to well-studied and well-dated events and processes indicative of climatic and environmental change (e.g., terrestrial, marine, and atmospheric records).

As expected, calibration increases the age of each data point and the weighted means associated with each layer (Table 8; Bard et al., 1990; Bard, 1998). Within the EUP, ages increase steadily with depth from 25,329 ± 363 cal BP$_{Hulu}$ (Layer 2) to 42,714 ± 805 cal BP$_{Hulu}$ (Layer 4d). The three subdivisions within Layer 4c are internally consistent and range from 34,704 ± 316 cal BP$_{Hulu}$ to 36,269 ± 344 cal BP$_{Hulu}$ to 39,475 ± 559 cal BP$_{Hulu}$, while the division between the LMP (Layer 5) and the EUP (Layer 4d) lies somewhere between 42,714 ± 805 cal BP$_{Hulu}$ and 42,860 ± 588 cal BP$_{Hulu}$. Without further sampling we can only consider this estimate as preliminary. Again, Layers 6 and 7 are indistinguishable at 45,872 ± 824 and 46,727 ± 1818 cal BP$_{Hulu}$, respectively.

Figure 8 combines TL and AMS (uncalibrated and calibrated) estimates on four timescales (^{14}C BP, cal BP$_{Hulu}$, cal BC) linked to the GRIP Ice Core record (ka BP$_{GRIP-Hulu}$). Chronometric data from Ortvale Klde are correlated with global paleoclimatic proxies, including modest warm oscillations (Greenland Interstadials: GI 1–17), and extreme cold periods (Heinrich events: H0–H6). The patterns observed within the radiocarbon calibration record of CalPal-2007$_{Hulu}$ indicate that Layers 2–4b span a period between H2 and H3, while Layer 4c represents a period that includes H4 and GI 9–7. As in Fig. 7, the pink dotted line in Fig. 8 indicates the oldest possible estimate for the Middle to Upper Paleolithic boundary at Ortvale Klde (~38 ka ^{14}C BP; 42.8 ka cal BP$_{Hulu}$), while the pink bar indicates the age range during which this replacement can be dated (~38 ka and ~34 ka ^{14}C BP; 42.8 ka cal BP$_{Hulu}$ and 41.6 ka cal BP$_{Hulu}$). This age range is determined based on several criteria including the precise stratigraphic position of each sample and the dates from Layers 5 and 4d. The Middle to Upper Paleolithic replacement event is correlated with a relatively sharp "boundary" at around GI 10. Layer 5 can be associated with GI 11 while Layers 6 and 7 correspond to GI 12. Layers 9 and 10 appear to span GI 13 and GI 14.

Interregional chronometric record

There are currently no other well-dated LMP–EUP sites in the southern Caucasus available for comparison with Ortvale Klde. Bronze Cave, located approximately 35 km southwest of Ortvale Klde, near the Imeretian village of Tsutskhvati, represents one of a series of Middle Paleolithic localities known collectively as the

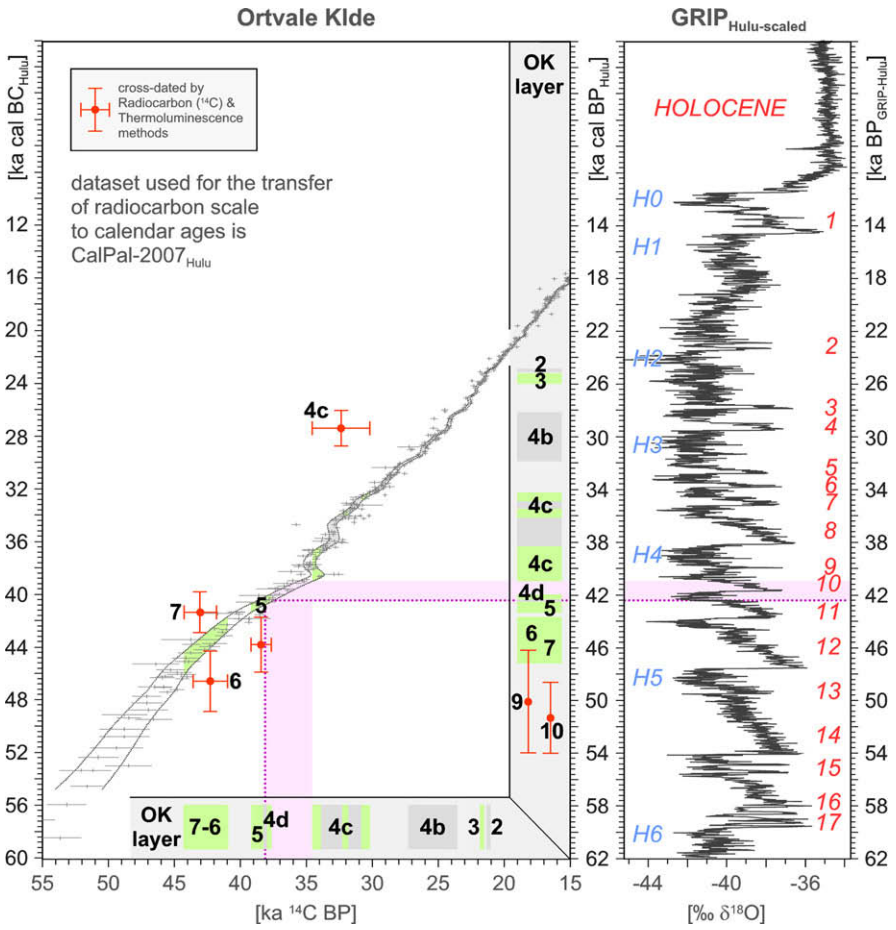

Fig. 8. Conversion of radiocarbon measurements from Ortvale Klde to calendar ages (cal BC/BP; see "Method" below), compared with the paleoclimate signatures (‰ $d^{18}O$) recorded in the Greenland "GRIP" Ice Core, scaled on the $Greenland_{Hulu}$-age-model ($BP_{GRIP\text{-}Hulu}$; cf. Weninger and Jöris, this issue). Modest warm interstadial oscillations are labeled in red and span GI 1 (Greenland Interstadial), the Late Glacial interstadial complex, through GI 16/17 (~58.0 $BP_{GRIP\text{-}Hulu}$; ~56.0 ka cal BC). Extreme cold (Heinrich) events recorded in the North Atlantic are labeled in light blue and span H0 (Younger Dryas) to H6 (the end of the 1st maximum cold of the last glacial cycle). Method: Most likely radiocarbon age-estimates (dark grey bars) and weighted means (green bars) from Fig. 7 are plotted on the radiocarbon time-scale and transferred to calendar ages (cal BC/BP) using the $CalPal\text{-}2007_{Hulu}$ calibration data set in the center of the left diagram (www.calpal.de; cf. www.calpal-online.de). Thermoluminescence (TL) estimates for Layers 4c–7 are indicated in red and are plotted at 1σ. Calendric age estimates for Layers 9 and 10 are based on TL dating only. As in Fig. 7, the pink dotted line indicates the oldest possible estimate for the Middle to Upper Paleolithic boundary at Ortvale Klde (~38.0 ka ^{14}C BP), while the pink bar indicates the age range during which this "transition" can be dated (~38.0 and ~34.5 ka ^{14}C BP). This age range is determined based on several criteria including the precise stratigraphic position of each sample and the dates from Layers 5 and 4d. The patterns observed within the radiocarbon calibration record of $CalPal\text{-}2007_{Hulu}$ "translate" the entire time-span of the Middle to Upper Paleolithic "transition" into a relatively sharp "boundary" at around GI 10.

Tsutskhvati complex; each site is attributed to the Tsutskhvati-type Mousterian (Liubin, 1977, 1989; Tushabramishvili, 1978). At Bronze Cave, the largest member of the complex, 24 lithological layers were defined (~18 m thick), within which five Middle Paleolithic layers were identified (Tushabramishvili, 1978). No Upper Paleolithic occupations were encountered. Available stratigraphic, paleontological, and archaeological data are summarized in Adler and Tushabramishvili (2004).

Attempts to date Bronze Cave began in 2001 with the collection of bone ($n = 8$) and charcoal ($n = 12$) samples from preserved

Table 10
AMS Data for Bronze Cave[a]

Lab#	Layer	Archaeology	Row	Material	Elevation	$\delta^{13}C$ ‰ PDB	^{14}C Age BP ± 1σ	Age Cal BP_{Hulu} ± 1σ
RTT 4222	14	MP 1	11	charcoal	na	−26.2	36700 ± 800	41664 ± 531
RTT 4223	14	MP 1	11	charcoal	na	−24.2	22900 ± 200	27512 ± 438
RTT 4229	14	MP 1	?	charcoal	na	−24.0	>45000	na
RTT 4221	15	MP 1	11	charcoal	na	−25.1	29700 ± 360	33944 ± 367
RTT 4224	15	MP 1	10?	charcoal	na	−24.4	34500 ± 600	39722 ± 919
RTT 4225	15	MP 1	10?	charcoal	na	−26.9	39500 ± 1200	43528 ± 904
RTT 4226	18	MP 2	10?	charcoal	na	−21.2	46300 ± 2600	50427 ± 3482
RTT 4227	18	MP 2	?	charcoal	na	−22.8	41600 ± 1400	45235 ± 1437
RTT 4228	18	MP 2	?	charcoal	na	−21.2	>45000	na
RTT 4230	20	MP 3	?	charcoal	na	−23.5	>45000	na
RTT 4231	20	MP 3	?	charcoal	na	−24.5	43500 ± 2000	47271 ± 2313
RTT 4232	20	MP 3	?	charcoal	na	−24.6	34200 ± 1200	38927 ± 1657

[a] Abbreviations: RTT = Weizmann Institute of Science; MP = Middle Palaeolithic. Data calibrated with CalPal-online (Danzeglocke, U., Jöris, O., Weninger, B., 2007. CalPal-2007online. http://www.calpal-online.de/).

stratigraphic sections by D. S. Adler and N. Tushabramishvili. Great pains were taken to record sample context but certain data (e.g., elevation, excavation unit) proved impossible to collect due to the eroded condition of the sections. Likewise attempts were made to extract datable specimens from several inches into the preserved sections rather than the face. Specimens of burned flint ($n = 10$) were also selected from collections curated at the Georgian State Museum. Thus far, only the charcoal specimens have been processed and dated and these do not provide a coherent suite of dates (Table 10). At present we believe the ambiguity associated with these data result from a combination of small sample size, the ephemeral nature of the Middle Paleolithic occupations, the dynamic taphonomic history of the site, the artificially thick archaeological horizons, and perhaps sample contamination. At best, we can propose that the Middle Paleolithic occupations at Bronze Cave are generally contemporaneous with those at Ortvale Klde, but the degree to which they are strictly contemporaneous cannot be estimated.

Dzudzuana Cave, located approximately 5 km east of Ortvale Klde, contains an Upper Paleolithic sequence that begins at ~32 ka ^{14}C BP (Layer D) and contains lithic and faunal material largely indistinguishable from that found in the EUP layers of Ortvale Klde (Meshveliani et al., 2004; Adler et al., 2006a; Bar-Yosef et al., 2006; Bar-Oz et al., 2008). At present no Middle Paleolithic deposits have been discovered. The EUP sequence at Dzudzuana ends at ~20 ka ^{14}C BP. Thus, the only reliable chronometric data on the replacement

Table 11
Chronometric results from Mezmaiskaya Cave[a]

Culture	Layer	Lab#	Method	Material	Age ^{14}C BP ± 1σ Age BP_{ESR} ± 1σ	t-value	Weighted Mean	Age Cal BP_{Hulu} ± 1σ	t-value	Weighted Mean
EPP/LUP	1A	AA-41855	AMS	bone	28510 ± 850	na	28510 ± 850	33023 ± 765	0.00	33023 ± 765
LUP	1B	CURL-5757	AMS	wood charcoal	32000 ± 250	0.97	32278 ± 138	36078 ± 383	0.60	36372 ± 310
		CURL-5756	AMS	wood charcoal	32400 ± 240	0.44		36937 ± 752	0.69	
		CURL-5759	AMS	wood charcoal	32400 ± 230	0.46		36935 ± 747	0.70	
EUP	1C	Beta-113536	AMS	wood charcoal	32010 ± 250	2.7	32766 ± 127	36095 ± 390	1.47	36799 ± 276
		CURL-5762	AMS	wood charcoal	33000 ± 260	0.81		37473 ± 675	0.92	
		CURL-5760	AMS	wood charcoal	33000 ± 240	0.86		37475 ± 665	0.94	
		CURL-5761	AMS	wood charcoal	33100 ± 270	1.12		37569 ± 689	1.04	
		GIN-10946	^{14}C	bone	32900 ± 900	0.35	33325 ± 838	37583 ± 1350	0.36	38228 ± 1166
		AA-41856	AMS	bone	36100 ± 2300	1.13		40128 ± 2317	0.73	
MP	2	LE-4735	AMS	bone	32230 ± 740	0.17	32401 ± 672	36730 ± 1123	0.20	37027 ± 990
		AA-41857	AMS	bone	33200 ± 1600	0.46		38063 ± 2097	0.45	
		GIN-10944	^{14}C?	bone	>35000	na	>35000	na	na	na
		RT61A	ESR	bovid: premolar	*EU: 36400 ± 2700* LU: 36900 ± 2700	*1.11* *0.75*	*EU: 39887 ± 1607*	na	na	na
		RT61B	ESR	premolar	*EU: 41800 ± 2000* LU: 42300 ± 2000	1.11 0.75	LU: 40387 ± 1607	na	na	na
	2A	Beta-53896/ CAMS-2999	??	burned bone	35760 ± 400	0.36	35944 ± 321	40633 ± 861	0.74	41329 ± 362
		Beta-53897/ ETH-9817	??	burned bone	36280 ± 540	0.52		41478 ± 399	0.28	
		CT50	ESR	*C. elaphus*: molar	EU: 40100 ± 1700 LU: 40800 ± 1700	na	EU: 40100 ± 1700 LU: 40800 ± 1700	na	na	na
	2B1	RT17	ESR	cervid: molar	EU: 36600 ± 2500 LU: 38400 ± 2600	na	EU: 36600 ± 2500 LU: 38400 ± 2600	na	na	na
	2B2	LE-3599	AMS	bone	40660 ± 1600	na	40660 ± 1600	44451 ± 1374	0.00	44451 ± 1374
	2B3	RT98	ESR	*Bison sp*: molar	*EU: 62900 ± 4800* LU: 64300 ± 5100	*1.91* *1.16*	*EU: 52375 ± 2719*	na	na	na
		RT97	ESR	bovid/cervid: molar	*EU: 47400 ± 3300* LU: 48700 ± 3400	1.85 1.09	LU: 53500 ± 2829	na	na	na
	2B4	RT93	ESR	*C. elaphus*: molar	EU: 68000 ± 5700 LU: 69700 ± 6000	na	EU: 68000 ± 5700 LU: 69700 ± 6000	na	na	na
		CT53	ESR	*Bison sp*: molar	*EU: 51700 ± 3300* LU: 57500 ± 3900	*0.47* *0.38*	*EU: 49877 ± 1982* LU: 58603 ± 2479	na	na	na
		CT56	ESR	*Bison sp*: molar	*EU: 48500 ± 3000* LU: 55200 ± 3800	*0.06* 1.71		na	na	na
		RT88	ESR	*Bison sp*: molar	*EU: 49600 ± 4400* LU: 53400 ± 5100	0.24 0.75		na	na	na
		CT57	ESR	bovid/cervid: molar	EU: 63600 ± 6700 LU: 70600 ± 7400	na	EU: 63600 ± 6700 LU: 70600 ± 7400	na	na	na
	3	Ua-14512	AMS	Neanderthal: rib	29195 ± 965	na	29195 ± 965	33451 ± 830	0.00	33451 ± 830
		LE-3841	AMS	bone	>45000	na	>45000	na	na	na
Sterile	4–7	na	na	na	na	na	na	na	na	na

[a] Abbreviations: EPP, Epipalaeolithic; LUP, Late Upper Palaeolithic; EUP, Early Upper Palaeolithic; MP, Middle Palaeolithic; EU, Early Uptake; LU, Linear Uptake. Labs: AA, National Science Foundation Arizona AMS Laboratory; Beta, Beta Analytic, Inc; CT and RT, Williams College; CURL, NSTAAR Laboratory for AMS Radiocarbon Preparation and Research (NSRL); GIN, Geological Institute RAS in Moscow; LE, St Petersburg; Ua, University of Uppsala. Data calibrated with CalPal-online (Danzeglocke, U., Jöris, O., Weninger, B., 2007. CalPal-2007online. http://www.calpal-online.de/). ESR samples CT53, CT56, RT88 appear to be derived from a single tooth row. All data are taken from Golovanova et al. (1999), Ovchinnikov et al. (2000), Skinner et al. (2005), Cleghorn (2006), and Golovanova et al. (2006).

of the LMP by the EUP in the southern Caucasus is limited to that described here from Ortvale Klde. The Dzudzuana team is currently continuing their excavations in search of LMP occupations at the site.

A new and growing series of chronometric data is now available from Mezmaiskaya Cave, located roughly 400 km northwest of Ortvale Klde on the northern side of the Caucasus Mountains (Table 11). The site is notable as the source of one of the first Neandertal specimens to be sequenced for MtDNA (Ovchinnikov et al., 2000). The single direct date of the Neandertal infant from Layer 3 ($29{,}195 \pm 965$ ^{14}C BP; Ovchinnikov et al., 2000) is not corroborated by numerous independent measurements (e.g., Golovanova et al., 1999; Golovanova and Doronichev, 2003; Skinner et al., 2005; Cleghorn, 2006; Golovanova et al., 2006). The shallow depth of the burial ($\leq$40 cm below the truncated surface) and its location at the front of the cave likely facilitated contamination of the bone collagen. The burial is located within a taphonomically active part of the cave where the stratigraphic situation is not well-understood. Better chronometric data is available from specimens collected deeper in the cave during recent excavations.

AMS bone ages (weighted mean: $33{,}325 \pm 838$ ^{14}C BP; $38{,}228 \pm 1{,}166$ cal BP$_{\text{Hulu}}$) are available for the EUP (Layer 1C), while four charcoal specimens provide a weighted mean of $32{,}766 \pm 127$ ^{14}C BP ($36{,}799 \pm 276$ cal BP$_{\text{Hulu}}$). The LMP (Layer 2) has been dated via AMS and ESR. The AMS results on bone provide a weighted mean of $32{,}401 \pm 672$ ^{14}C BP ($37{,}027 \pm 990$ cal BP$_{\text{Hulu}}$). Based on Skinner et al. (2005) two ESR estimates date the LMP (Layer 2) to between 39.9 ± 1.6 ka BP$_{\text{ESR}}$ (weighted mean, early uptake) and 40.4 ± 1.6 ka BP$_{\text{ESR}}$ (weighted mean, linear uptake). Thus, the true age of the Neandertal burial appears to have been seriously underestimated in Ovchinnikov et al. (2000).

The available data allow us to estimate the start of the EUP of Mezmaiskaya Cave at $\sim$33 ka ^{14}C BP ($\sim$38–37 ka cal BP$_{\text{Hulu}}$) and the end of the LMP at $\sim$32 ka ^{14}C BP ($\sim$37 ka cal BP$_{\text{Hulu}}$) and $\sim$40 ka BP$_{\text{ESR}}$. Comparison of the calibrated radiocarbon data from Mezmaiskaya Cave and Ortvale Klde indicate that statistically (i.e., $>$2 sigma) the replacement events at the two sites are not contemporaneous and may be separated by several thousand calibrated radiocarbon years. This separation ceases when one compares the radiocarbon and ESR data, and we predict that with continued dating in the Caucasus this gap will disappear entirely. While the lack of key contextual information limits our ability to critically evaluate the published Mezmaiskaya Cave dataset in a manner similar to that outlined above, comparisons with Ortvale Klde suggest an initial EUP expansion into the southern Caucasus, followed quickly in time by expansion along the Black Sea coast and into the northern Caucasus.

Conclusions

The analyses conducted here are designed to help cull aberrant or otherwise problematic data from the chronometric record of Ortvale Klde in an attempt to provide a more rigorous temporal estimate for the Middle to Upper Paleolithic replacement event at the site and within the southern Caucasus. Implementation of our discard protocol resulted in the rejection of 25% of the dated samples. More importantly, this procedure increased our confidence in the quality and reliability of the remaining data and allow us to estimate the oldest possible age for the boundary between the Middle and Upper Paleolithic at $\sim$38 ka ^{14}C BP (42.8 ka cal BP$_{\text{Hulu}}$), with a conservative estimate between $\sim$38 ka and $\sim$34 ka ^{14}C BP (42.8 ka cal BP$_{\text{Hulu}}$ and 41.6 ka cal BP$_{\text{Hulu}}$). This age range is determined based on criteria outlined above and allows us to correlate the end of the LMP and the beginning of the EUP with a relatively sharp boundary at GI 10, with the LMP ascribed to GI 11.

While detailed comparison with neighboring sites in the southern Caucasus is problematic, several general conclusions regarding the demise of the Neandertals are possible. At present there do not appear to be any LMP sites within the region younger than $\sim$38 ka ^{14}C BP, and we predict that ongoing research within the region (sensu stricto) will not alter this observation in any significant way. In our view, the end of the LMP and the beginning of the EUP in the southern Caucasus marks a rapid population replacement event in which the Neandertals disappeared in the face of expanding modern humans. This paper addresses the timing of the replacement while elsewhere we have discussed the archaeological and behavioral fallout (Adler, 2002; Adler et al., 2006a,b; Bar-Yosef et al., 2006). In summary, we find that while both populations appear to have subsisted on the same prey species (*Capra caucasica*), the Neandertals did so within small territories and so had limited contacts with neighboring groups. The same lithic raw material data indicate that the EUP populations who replaced the Neandertals routinely exploited much larger territories and suggest an ability to construct, navigate, and maintain larger social networks. Research on the northern side of the Caucasus, best represented by that conducted at Mezmaiskaya Cave, correlate well both archaeologically and chronometrically with data from Ortvale Klde and suggest that the demise of the Neandertals occurred rapidly in both regions as part of the same demographic process of population expansion and replacement.

Acknowledgements

The authors wish to thank their colleagues at the Georgia State Museum, in particular Dr. D. Lordkipanidze (Director), Dr. A. Vekua, Dr. T. Meshveliani, and Dr. N. Jakeli for many years of fruitful collaboration. D. S. Adler thanks the Wenner-Gren Foundation for Anthropological Research (Grants 6881 and 7059), the L. S. B. Leakey Foundation, the American School of Prehistoric Research at Harvard University, and the Davis Center for Russian Studies at Harvard University for their generous financial support for fieldwork and analyses. O. Bar-Yosef is grateful to the American School of Prehistoric Research at Harvard University for financial support of the Dzudzuana Cave project. Finally, thanks are due to O. Jöris and anonymous reviewers who provided thoughtful comments on earlier drafts of this text.

References

Adamiec, G., Aitken, M.J., 1998. Dose-rate conversion factors: update. Ancient TL 16, 35–70.

Adler, D.S., 2002. Late Middle Paleolithic patterns of lithic reduction, mobility, and land use in the southern Caucasus. Ph.D. Dissertation, Harvard University.

Adler, D.S., Bar-Oz, G., Belfer-Cohen, A., Bar-Yosef, O., 2006a. Ahead of the game: Middle and Upper Paleolithic hunting practices in the southern Caucasus. Curr. Anthropol. 47, 1–35.

Adler, D.S., Belfer-Cohen, A., Bar-Yosef, O., 2006b. Between a rock and a hard place: Neandertal-modern human interactions in the southern Caucasus. In: Conard, N.J. (Ed.), Neandertals and Modern Humans Meet. Publications in Prehistory. Kerns Verlag, Tübingen, pp. 165–187.

Adler, D.S., Tushabramishvili, N., 2004. Middle Paleolithic patterns of settlement and subsistence in the southern Caucasus. In: Conard, N.J. (Ed.), Middle Paleolithic Settlement Dynamics. Publications in Prehistory. Kerns Verlag, Tübingen, pp. 91–132.

Anikovich, M.V., Sinitsyn, A.A., Hoffecker, J.F., Holliday, V.T., Popov, V.V., Lisitsyn, S.N., Forman, S.L., Levkovskaya, G.M., Pospelova, G.A., Kuzmina, I.E., Burova, N.D., Goldberg, P., Macphail, R.I., Giaccio, B., Praslov, N.D., 2007. Early Upper Paleolithic in Eastern Europe and implications for the dispersal of modern humans. Science 315, 223–315.

Bard, E., 1998. Geochemical and geophysical implications of the radiocarbon calibration. Geochim. Cosmochim. Acta 62, 2025–2038.

Bard, E., Hamelin, B., Fairbanks, R.G., Zindler, A., 1990. Calibration of the ^{14}C timescale over the past 30,000 years using mass spectrometric U-Th ages from Barbados corals. Nature 345, 405–410.

Bar-Oz, G., Adler, D.S., 2005. The taphonomic history of the Middle and Upper Paleolithic faunal assemblages from Ortvale Klde, Georgian Republic. J. Taphonomy 3, 185–211.

Bar-Oz, G., Belfer-Cohen, A., Meshvekiani, T., Djakeli, N., Bar-Yosef, O., 2008. Taphonomy and zooarchaeology of the Upper Palaeolithic Cave of Dzudzuana, Republic of Georgia. Int. J. Osteoarchaeol. 18, 131–151.

Bar-Yosef, O., 1998. On the nature of transitions: the Middle to Upper Paleolithic and the Neolithic revolution. Cambridge Archaeol. J. 8, 141–163.
Bar-Yosef, O., 2001. Dating the transition from the Middle to Upper Paleolithic. In: Barrandon, J.-N., Guibert, P., Michel, V. (Eds.), Datation. XXIe rencontres internationals d'archeologie et d'histoire d'Antibes. Editions APDCA, Antibes, pp. 279–293.
Bar-Yosef, O., Belfer-Cohen, A., Adler, D.S., 2006. The implications of the Middle-Upper Paleolithic chronological boundary in the Caucasus to Eurasian prehistory. Anthropologie XLIV, 49–60.
Bocquet-Appel, J.-P., Demars, P.-Y., 2000. Neandertal contraction and modern human colonization of Europe. Antiquity 74, 544–552.
Brennan, B.J., Rink, W.J., McGuirl, E.L., Schwarcz, H.P., Prestwich, W.V., 1997. Beta doses in tooth enamel by "One-Group" theory and the ROSY ESR dating software. Radiation Measurements 27, 307–314.
Bronk Ramsey, C., Buck, C.E., Manning, S.W., Reimer, P., van der Plicht, H., 2006. Developments in radiocarbon calibration for archaeology. Antiquity 80, 783–798.
Bronk Ramsey, C., Higham, T., Bowles, A., Hedges, R., 2004. Improvements to the pretreatment of bone at Oxford. Radiocarbon 46, 155–163.
Cleghorn, N.E., 2006. A zooarchaeological perspective on the Middle to Upper Paleolithic transition at Mezmaiskaya Cave, the northwestern Caucasus, Russia. Ph.D. Dissertation, Stony Brook University.
Cohen, V., Stepanchuk, V.N., 1999. Late Middle and early Upper Paleolithic evidence from the East European plain and Caucasus: a new look at variability, interactions, and transitions. J. World Prehist. 13, 265–319.
Conard, N.J., Bolus, M., 2003. Radiocarbon dating the appearance of modern humans and timing of cultural innovations in Europe: new results and new challenges. J. Hum. Evol. 44, 331–371.
d'Errico, F., 2003. The invisible frontier. A multiple species model for the origin of behavioral modernity. Evol. Anthropol. 12, 188–202.
Doronichev, V.B., 1993. Mustierskie industrii Bol'shogo kavkaza (The Mousterian Industries of the Great Caucasus). Peterburgurskiy Arkheologicheskiy Vestnik (St. Petersburg Archaeology News) 7, 14–24.
Golovanova, L.V., Cleghorn, N., Doronichev, V.B., Hoffecker, J.F., Burr, G.S., Sulergizkiy, L.D., 2006. The early Upper Paleolithic in the northern Caucasus (New data from Mezmaiskaya Cave, 1997 excavation). Eurasian Prehist. 4 (1–2), 43–78.
Golovanova, L.V., Doronichev, V.B., 2003. The Middle Paleolithic of the Caucasus. J. World Prehist. 17, 71–140.
Golovanova, L.V., Hoffecker, J.F., Kharitonov, V.M., Romanova, G.P., 1999. Mezmaiskaya Cave: a Neandertal occupation in the northern Caucasus. Curr. Anthropol. 40, 77–86.
Higham, T., Bronk Ramsey, C., Karavanic, I., Smith, F.H., Trinkaus, E., 2006a. Revised Direct Radiocarbon Dating of the Vindija G1 Upper Paleolithic Neandertals. Proc. Natl. Acad. Sci. 103, 553–557.
Higham, T.F.G., Jacobi, R.M., Bronk Ramsey, C., 2006b. AMS radiocarbon dating of ancient bone using ultrafiltration. Radiocarbon 48, 179–195.
Jacobi, R.M., Higham, T.F.G., 2008. The 'Red Lady' ages gracefully: New ultrafiltration AMS determinations from Paviland. J. Hum. Evol. 55, 898–907.
Lioubine, V.P., 2002. L'Acheuléen du Caucase. ERAUL 93. Université de Liège, Liège.
Liubin, V.P., 1977. Mustierskie kul'turi Kavkaza (Mousterian Cultures of the Caucasus). Nauka, Leningrad.
Liubin, V.P., 1989. Paleolit Kavkaza (Paleolithic of the Caucasus). In: Boriskovski, P.I. (Ed.), Paleolit Kavkaza i Sredney Azii (The Paleolithic of the Caucasus and Northern Asia). Nauka, Leningrad, pp. 9–144.
Liubin, V.P., Tcherniachovski, A.G., Barychnikov, G.F., Levkovskaia, G.M., Selivanova, N.B., 1985. La Grotte de Koudaro I (Résultats de Recherches Pluridisciplinaires). L'Anthropologie 89, 159–180.
Mercier, N., Valladas, H., Valladas, G., 1992. Observations on palaeodose determination with burnt flints. Ancient TL 10, 28–32.
Meshveliani, T., Bar-Yosef, O., Belfer-Cohen, A., 2004. The Upper Paleolithic of Western Georgia. In: Brantingham, P.J., Kuhn, S.L., Kerry, K.W. (Eds.), The Early Upper Paleolithic Beyond Western Europe. University of California Press, Berkeley, pp. 129–143.
Millard, A.R., 2008. A critique of the chronometric evidence for hominid fossils: I. Africa and the Near East 500–50 ka. J. Hum. Evol. 54, 848–874.
Ovchinnikov, I.V., Götherström, A., Romanova, G.P., Kharitonov, V.M., Lidén, K., Goodwin, W., 2000. Molecular analysis of Neandertal DNA from the northern Caucasus. Nature 404, 490–493.
Pettitt, P.B., Davies, W., Gamble, C.S., Richards, M.B., 2003. Paleolithic radiocarbon chronology: quantifying our confidence beyond two half-lives. J. Archaeol. Sci. 30, 1685–1693.
Rink, W.J., Grün, R., Yalçinkaya, I., Otte, M., Taskiran, H., Valladas, H., Mercier, N., Bar-Yosef, O., Koslowski, J., Schwarcz, H.P., 1994. ESR dating of the Last Interglacial Mousterian at Karaïn Cave, southern Turkey. J. Archaeol. Sci. 21, 839–849.
Skinner, A.R., Blackwell, B.A.B., Martin, S., Ortega, A., Blickstein, J.I.B., Golovanova, L.V., Doronichev, V.B., 2005. ESR dating at Mezmaiskaya Cave, Russia. Appl. Radiat. Isot. 62, 219–224.
Spriggs, M., 1989. The dating of the island Southeast Asian Neolithic: an attempt at chronometric hygiene and linguistic correlation. Antiquity 63, 587–613.
Spriggs, M., Anderson, A., 1993. Late colonisation of East Polynesia. Antiquity 67, 200–217.
Tushabramishvili, D.M. (Ed.), 1978. Arkheologicheskie panyatniki Tsutskhvatskogo mnogoetajnogo peshernogo kompleska (Archaeological Sites of the Tsutskhvati Cave Complex). Metsniereba, Tbilisi.
Tushabramishvili, N., 1994. Srednii Paleolit Zapadnoi gruzii i etapy ego perekhoda k verkhnemu paleolitu (po materialam Ortvala-Klde) (The Middle Paleolithic of Western Georgia and the stages of its transition to the Upper Paleolithic based on material from Ortvale Klde). Ph.D. Dissertation, University of Tbilisi.
Tushabramishvili, N., Lordkipanidze, D., Vekua, A., Tvalcherlidze, M., Muskhelishvili, A., Adler, D.S., 1999. The Middle Paleolithic rockshelter of Ortvale Klde, Imereti Region, the Georgian Republic. Préhistoire Europeenne 15, 65–77.
Valladas, G., Valladas, H., 1982. Effet de l'irradiation alpha sur des grains de quartz. A specialist seminar on thermoluminescence dating. PACT 6, 171–178.
Valladas, H., 1992. Thermoluminescence dating of flint. Quatern. Sci. Rev. 11, 1–5.
van Andel, T.H., 2005. The ownership of time: approved ^{14}C calibration or freedom of choice? Antiquity 79, 944–948.
van Andel, T.H., Davies, W. (Eds.), 2003. Neandertals and Modern Humans in the European Landscape During the Last Glaciation. McDonald Institute for Archaeological Research, Cambridge.
Weninger, B., Jöris, O., 2008. A 14C age calibration curve for the last 60 ka: The Greenland-Hulu U/Th time-scale and its impact on understanding the Middle to Upper Paleolithic transition in Western Eurasia. In: Adler, D.S., Jöris, O. (Eds.), Setting the Record Straight: Toward a Systematic Chronological Understanding of the Middle to Upper Paleolithic Boundary in Eurasia. J. Hum. Evol. 55, this issue.
Yizhaq, M., Genia Mintz, G., Cohen, I., Khalaily, H., Weiner, S., Boaretto, E., 2005. Quality controlled radiocarbon dating of bones and charcoal from the early pre-pottery Neolithic B (PPNB) of Motza (Israel). Radiocarbon 47, 193–206.
Zilhão, J., 2006. Genes, Fossils, and Culture. An Overview of the Evidence for Neandertal-Modern Human Interaction and Admixture. Proc. Prehist. Soc. 72, 1–20.
Zilhão, J., d'Errico, F., 1999. The chronology and taphonomy of the earliest Aurignacian and its implications for the understanding of Neandertal extinction. J. World Prehist. 13, 1–68.